Advances in Applied Mathematics and Mechanics
Adv. Appl. Math. Mech., Vol. **17**, No. 4, pp. 1171-1203

DOI: 10.4208/aamm.OA-2023-0327
August 2025

Stokes Flows Imposed Constant Navier Slip Length on Boundary for Domains of Simple Geometry

Zhan-Rui Qiu and Wei-Dong Su*

State Key Laboratory for Turbulence and Complex Systems and Department of Mechanics and Engineering Science, College of Engineering, Peking University, Beijing 100871, China

Received 22 December 2023; Accepted (in revised version) 20 June 2024

Abstract. In micro-nano and even some macro-scale flows, the boundary slip cannot be ignored and has an important influence. We consider the most widely used Navier slip length model to investigate whether the solution of Stokes flow exists if a homogeneous slip is imposed as a boundary condition replacing the ordinary Dirichlet condition of velocity for some domains of simple geometries, including the two-dimensional channel, plane annulus and axisymmetric circular pipe. The Fourier series is employed to obtain the exact solutions formulated by the stream function. While a unique solution exists for most cases, it is found that yet occurs the cases of no solution under a certain slip length and infinitely multiple solutions under an infinitely discrete set of slip lengths, respectively.

AMS subject classifications: 76D07, 31A30, 35J40

Key words: Stokes flow, boundary condition, slip length, no solution, multiple solution.

1 Introduction

People tended to believe that there is a non-slip boundary condition on the solid-fluid surface in early years. In 1738, Bernoulli [1] first proposed the non-slip boundary condition, which refers to that the relative velocity between the fluid and the neighbouring solid surface is zero. But with in-depth research the non-slip condition has been questioned by some people. In 1823, Navier [2] put forward an assumption of linear slip boundary condition that the slip velocity is proportional to the local shear deformation rate, which in the simplest flow conditions can be expressed as

$$v_b = \ell \frac{\partial v_b}{\partial n}, \tag{1.1}$$

*Corresponding author.
Email: swd@pku.edu.cn (W.-D. Su)

 ©2025 Global Science Press

where v_b is the relative slip velocity of the fluid on the solid boundary, ℓ is the slip length and n is the normal direction of the boundary pointing towards the fluid. Debye [3] verified the existence of slip boundary in experiment. With the development of micro-nano technology in modern times, more detailed studies have been carried out on the boundary conditions of fluid flow [4–8]. It is found that the boundary slip of dense fluid flow does exist under some conditions, and has an important impact on the global hydrodynamic behaviour [8–10]. It is also found that the slip length is usually positive on the superhydrophobic surfaces [4, 5], while a negative slip length exists on the strong hydrophilic surfaces [5, 11] and even on some patterning hydrophobic surfaces with entrapped microbubbles [12].

At present, the application of slip boundary is very extensive, which mainly is studied through numerical and experimental research [9–22]. Furthermore, there are theoretical studies in fields of mathematics and fluid mechanics, especially on the question whether the Stokes and Navier-Stokes systems under Navier slip boundary condition is solvable or well-posed in a sense of mathematics [23–33]. For convenience in obtaining standard results, however, many works concentrated on weak solutions or limited slip length to some specific range. The first paper about existence problem is by Solonnikov and Scadilov [23], where they considered $\ell = \infty$ (full-slip). They proved the existence of weak solutions for the stationary Navier-Stokes system with external force. Amrouche and Rejaiba [24] proved the existence of weak solutions in a bounded domain with full-slip condition for nonsmooth data. In [25], Conca discussed the well-posedness of both linear and nonlinear problems with slip condition, assuming $\ell \geq 0$. Beirão Da Veiga [26] proved the existence of weak and strong solutions of generalized Stokes problem with $\ell \geq 0$ constant. Masmoudi and Rousset [33] proved the existence of a strong solution on an uniform interval of time in vanishing viscosity limit for the Navier-Stokes system with a Navier slip satisfying $|\ell| \geq 1$.

Recently, Acevedo et al [27, 28] and have studied the stationary Stokes and Navier-Stokes equations with inhomogeneous Navier boundary condition in three dimensional bounded domain. They proved the existence of a unique weak solution to the linear problem and obtained uniform estimates of the solutions for $\ell \geq 0$. Additionally, mathematical problems on more general slip conditions are also tackled in the background of modelling patterned or structured surfaces with or without roughness. Le Roux [29] proved that the Stokes problem has a unique weak solution with a general anisotropic Navier type slip boundary condition, wherein the slip length depends not only on the position but also on the direction of local velocity. Also, relevant studies for Non-Newtonian fluids emerge in recent years. For such fluids the slip length may depend nonlinearly on the wall shear stress. Baranovskii [30, 31] investigated the existence of weak solutions for 3D steady flows of different types in a bounded domain under threshold-slip boundary conditions. Generally, the slip length ℓ is assumed to be nonnegative in order to ensure the conservation of energy. However, mathematically speaking, it is also reasonable to take a negative value for ℓ [32, 33].

As we know, for the interior problem, Laplace equation has the uniqueness theorem

with Robin boundary condition of the form $\partial v/\partial n+tv=0$ similarly to Navier slip condition when $t>0$. Without this condition, there is no general uniqueness theorem [34]. Additionally, for Laplace equation in periodic channel under inhomogeneous Robin conditions on both sides, as long as the Robin condition parameter t on one side of the boundary is negative, no matter whether the parameter on the other side is positive or negative, it is possible for the problem to have no solution or infinitely many solutions (see Appendix A). The possible non-uniqueness of the solution under slip length with variable sign may provide an explanation why there are always some limitations on slip length in the present mathematical works. The Stokes flow problem with homogeneous Navier slip boundary condition is similar to the Laplace equation with Robin boundary condition. In fact, it is well known that the Stokes equations is well-posed under the Dirichlet boundary condition respect to the velocity [35], and exact solutions can be obtained for some specific domains of simple geometry. Enlightened by the case of Laplace equation under Robin boundary condition, we want to know whether the similar non-uniqueness of solution may indeed be present for Stokes equations under constant but unlimited boundary slip. However, such exploration seems still absent, especially in the view from community of applied mathematics and mechanics. In this paper, we use the most popular Navier slip length as an imposed boundary condition to replace the Dirichlet condition of velocity on boundary for some canonical domains and investigate whether the Stokes flow can be uniquely determined.

In the above mentioned research, most of them focus on the well-posedness of the stationary Stokes problem with nonnegative slip condition and the nonstationary problem with negative slip condition, where the availability of the Gronwall's inequality simplifies the problem of the latter [32,33]. The main novelty of the present work is that we try to find the precise dependence of the solution of the Stokes problem on slip length ℓ for some specific cases. Compared with the existing works, we focus on the non-uniqueness of the stationary solution under ℓ with no limitation on its sign. As the first step in this line, the domains considered are all of simple geometry and the ℓ is assumed a constant and thus exact solutions can be obtained by means of Fourier series. In all of the cases we analysed, the Stokes problem no longer has a unique solution or even no solution for a certain set of slip length at different boundaries.

It should be emphasized that, once the well-posedness becomes focus more concerned, from mathematical point of view the generation mechanism for the possible homogeneous slip length on the boundary, i.e., whether it is due to the resting but slippery boundary or the active moving of a no-slip boundary, will not be distinguished any longer.

For plane Stokes flows, we introduce the stream function ψ, which satisfies the biharmonic equation

$$\Delta^2\psi=0. \tag{1.2}$$

The boundary conditions are then transformed into the form expressed by the stream

function, while the necessary flux condition on the inlet is added. These details are presented in the next section.

The domains studied include a two-dimensional channel, a plane annulus and an axisymmetric circular pipe. We present the results according to this classification in Section 2 and summarize the main results in Section 3. It is found that, once there exists the solutions for constant slip ℓ lying in some intervals, the solutions will be classical. The proof is given in Appendix B.

2 Stokes flows imposed constant slip length on boundary under typical geometry

2.1 Flow in a two-dimensional channel

As the first case we study a Stokes flow in a two-dimensional x-periodic channel domain ($0 \le x \le L$, $0 \le y \le d$) with the following both-side slip and additional one-side move condition

$$\begin{cases} \psi = 0, & \dfrac{\partial \psi}{\partial y} = \ell_0 \dfrac{\partial^2 \psi}{\partial y^2} & \text{at } y = 0, \\ \psi = C, & \dfrac{\partial \psi}{\partial y} = -\ell_d \dfrac{\partial^2 \psi}{\partial y^2} + V(x) & \text{at } y = d, \end{cases} \tag{2.1}$$

where C is a pre-set constant denoting the fluid volume flux through the channel, $V(x)$ is an additional variable boundary velocity. The x-axis, i.e., the totally streamwise direction, is parallel to the boundary of the channel. Due to the periodicity of the problem, all of the functions are supposed to be periodic with period L.

By terms of the Fourier expansion the stream function and boundary velocity can be expressed in the series form as

$$\psi(x,y) = a_0(y) + \sum_{n=1}^{\infty} \left[a_n(y) \cos\left(\frac{2\pi n x}{L}\right) + b_n(y) \sin\left(\frac{2\pi n x}{L}\right) \right], \tag{2.2a}$$

$$V(x) = V_0 + \sum_{n=1}^{\infty} \left[V_n \cos\left(\frac{2\pi n x}{L}\right) + W_n \sin\left(\frac{2\pi n x}{L}\right) \right], \tag{2.2b}$$

where V_0, V_n and V_m are coefficients of boundary velocity expansion, $a_0(y)$, $a_n(y)$ and $b_n(y)$ can be solved after substituting the above expression into the biharmonic equation that the stream function satisfies, i.e., Eq. (1.2). The results are listed as

$$a_0(y) = A_0 y^3 + B_0 y^2 + C_0 y + D_0, \tag{2.3a}$$

$$a_n(y) = (A_n + B_n y) e^{2\pi n y/L} + (C_n + D_n y) e^{-2\pi n y/L}, \tag{2.3b}$$

$$b_n(y) = (E_n + F_n y) e^{2\pi n y/L} + (G_n + H_n y) e^{-2\pi n y/L}, \tag{2.3c}$$

where those constants denoted by capital letters are undetermined coefficients depending on the boundary conditions, which can be treated properly as follows.

Firstly, we substitute Eq. (2.3a) into boundary condition Eq. (2.1) and compare each Fourier coefficient as the function of y, then we obtain

$$\begin{cases} D_0=0, \\ 2\ell_0 B_0 - C_0 = 0, \\ A_0 d^3 + B_0 d^2 + C_0 d = C, \\ 3(d^2+2\ell_d d)A_0 + 2(d+\ell_d)B_0 + C_0 = V_0. \end{cases} \tag{2.4}$$

The coefficient determinant of this linear algebraic equations can be given as $M_0=-4\ell_d d^3-4\ell_0 d^3-12\ell_0\ell_d d^2-d^4$. Clearly, when $\ell_0=-d/3$ or $\ell_d=-d/3$, we have $M_0=d^4/3\neq 0$. Conversely, when $\ell_0\neq -d/3$ and $\ell_d\neq -d/3$, we have $M_0=0$ if

$$\frac{4\ell_0}{d}+\frac{4\ell_d}{d}+\frac{12\ell_0\ell_d}{d^2}+1=0. \tag{2.5}$$

Therefore, in which case the Eq. (2.4) might have no solution when $(3d+6\ell_d)C\neq d^2V_0$, or infinitely many solutions when $(3d+6\ell_d)C=d^2V_0$. On the other hand, if ℓ_0 and ℓ_d do not satisfy the relation of Eq. (2.5), the Eq. (2.4) have the unique solution irrelevant to C and V_0.

Subsequently, we substitute Eqs. (2.3b) and (2.3c) into Eq. (2.1), and find that for each $a_n(y)$ and $b_n(y)$ an inhomogeneous linear algebraic equations follows with the right hand terms V_n and W_n respectively as well as the same coefficient determinant M_n. By calculation we conclude that, letting $M_n=0$, ℓ_0 and ℓ_d satisfy the following relations which depend on n, i.e.,

$$\begin{aligned} &\frac{\ell_0+\ell_d}{d}n_d[\sinh(n_d)-n_d]-\frac{\ell_0\ell_d}{d^2}n_d^2[1-\cosh(n_d)] \\ =&1-\cosh(n_d)+\frac{n_d^2}{2}, \quad \frac{n_d L}{4\pi d}=1,2,\cdots, \end{aligned} \tag{2.6}$$

where $n_d\equiv 4\pi d n/L$. The relations corresponding to a set of non-unique $a_n(y)$, $b_n(y)$, $c_n(y)$ and $d_n(y)$, i.e., the Stokes equations might have no solution or infinitely many solutions if the slip lengths (ℓ_0,ℓ_d) satisfy Eq. (2.6) for certain $n\in\mathbb{N}=\{1,2,3,\cdots\}$. It is found that there are at most two distinct n making $M_n=0$ at the same time. Therefore, there are at most two modes remained in Eq. (2.2a) when the multiple solutions occur. The detail on the zeros of M_n is presented in Appendix C. On the other hand, once a certain equation set has no solution, the whole problem has no solution. By checking the rank of the augmented matrix, it is found that, whether the non-uniqueness implies no solution or infinitely many solutions depends only on (V_n,W_n). If $(V_n,W_n)\neq(0,0)$, there is no solution; otherwise infinitely solutions.

We take different n with $d=1$ and $L=2\pi$ and then plot the curve of the relation between dimensionless slip lengths ℓ_0/d and ℓ_d/d in Fig. 1. The curve is central symmetric.

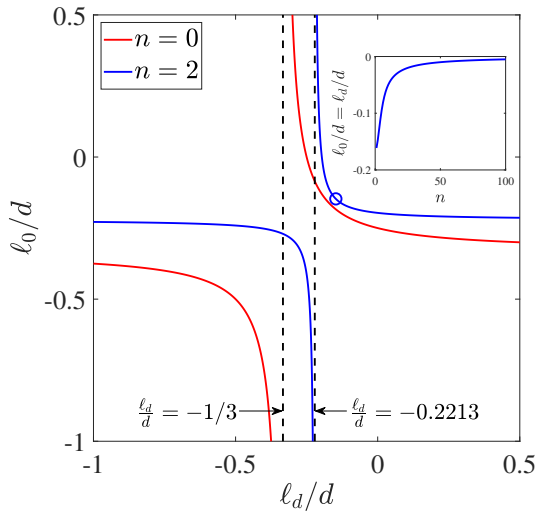

Figure 1: The (ℓ_0,ℓ_d) distribution leading to non-unique solution for Stokes flow imposed slip condition on the both sides boundary of a two-dimensional channel. On the curves, the coefficient determinant $M_n=0$. The plot is for two typical values of n. There are such cases that two curves for distinct n may intersect at two symmetric points, however, as shown in Appendix C.

At the same time, we find that the slip length ℓ_0 and ℓ_d are either both negative or one positive and one negative the same as the Laplace equation under Robin condition (see Appendix A). When the slip length of one side is positive, the slip length of the other side takes near the value of blue circle which shows $\ell_0/d=\ell_d/d$ in Fig. 1. Therefore, by observing the value of the blue circle with n, we find that the no solution problem corresponds to a set of small positive and negative slip lengths for large n.

In most situations, the determinant M_n does not vanishing for any $n\in\mathbb{N}$ and thus the problem has unique solution. Since the solution is represented usually by an infinite series, i.e., Eq. (2.2a), it is necessary to discuss the convergence of the series. Although the case of unique solution is not our major concern, a necessary argument on the regularity of the solution should be clarified. It is not difficult to prove that the series is uniformly convergent and moreover the unique solution is classical solution of the problem. Except the boundary regulating the velocity $V(x)$, on which the smoothness of the solution depends on degree of the smoothness of $V(x)$, the solution is actually C^∞ in otherwise part of the channel. We put the detail into Appendix B.

2.1.1 Two typical flows: Couette flow and Poiseuille flow

Through the analysis of Stokes flow under general boundary conditions, we find the equation might have no solution under the inhomogeneous condition, while it has multiple solutions under the homogeneous condition. In general boundary conditions, we use boundary moving velocity and flux conditions as inhomogeneous terms. When bound-

ary moving velocity vanishes, the flow corresponds to Poiseuille flow where the external parameter of the pressure gradient is specified by the value of the stream function, while when flux condition vanish, the flow corresponds to Couette flow with upper boundary move. Therefore, we will discuss these two typical flow as examples.

Firstly, when boundary moving velocity vanishing, i.e., $V(x)=0$, the slip boundary condition for Poiseuille flow becomes homogeneous and the equation set for $a_n(y)$ and $b_n(y)$ has infinitely many solutions if ℓ_0 and ℓ_d hold relation of the Eq. (2.6) and the rest terms for otherwise n are all zero. Conversely, all the $a_n(y)$ and $b_n(y)$ are zero. For $a_0(y)$, the same as mentioned above, the Eq. (2.4) without V_0 have the unique solution when ℓ_0 and ℓ_d satisfy relation of the Eq. (2.5). Conversely, it has no solution when Eq. (2.5) is tenable.

Then, we discuss the Couette flow with the appropriate boundary flux condition for the same inlet and outlet pressure distribution, i.e., $A_0=0$. For every n, the equation set may have the same inhomogeneous term, i.e., the expansion coefficient of boundary velocity V_0, V_n and W_n. Clearly, for any n, if ℓ_0 and ℓ_d satisfy the Eq. (2.5) or Eq. (2.6), and it happens that V_n or W_n vanishes, the equation set for $a_n(y)$ or $b_n(y)$ has infinitely many solutions, while V_n and W_n exist, the equation set might have no solution. On the contrary, when both of the Eq. (2.5) and Eq. (2.6) are not tenable, the flow problem has the unique solution.

The case of one side of positive slip length and one side of negative slip length might be more interesting, since for certain slip lengths the equation set might have multiple solutions or no solution, and the flow begin to display a variation along the streamwise. To observe the effect of positive slip length, we take a unique solution and some multiple solutions cases, i.e., $n=4$ with the appropriate slip lengths ℓ_0 and ℓ_d relation and then select one of the solutions for Poiseuille flow and Couette flow to plot the streamline distribution and the corresponding velocity and pressure profiles. The results are shown in Figs. 2-5. Due to the boundary driving and boundary slip, there are vortices in the flow field, which enhances the flow mixing; and the distance between the vortex centre and boundary depends on the values of n. In Figs. 2(b), (e), (f), when the slip lengths on both sides are equal, the flow has good symmetry with respect to the central axis of the channel (which can be more intuitively seen from the velocity and pressure profiles in Fig. 3). Especially Figs. 2(a), (c), (d) and Figs. 4(a), (c), (d), the upper boundary with a positive slip length affects the shape of the vortex and the pressure profiles in the flow field. In the Couette flow, the non-uniform motion of the upper boundary distorts the bottom vortex and disorder the original periodic vortex. Moreover, as the value of A_n increases, the spreading range or the thickness of the vortex can reach the whole channel (see Figs. 2(b), (d), (f)).

2.1.2 Constant slip length on single-side boundary

We find that for periodic channel with constant Navier slip conditions imposed on both sides of the boundary, there are no solution, infinitely many solutions or unique solutions in specific conditions and relations. Next, we study another situation in periodic chan-

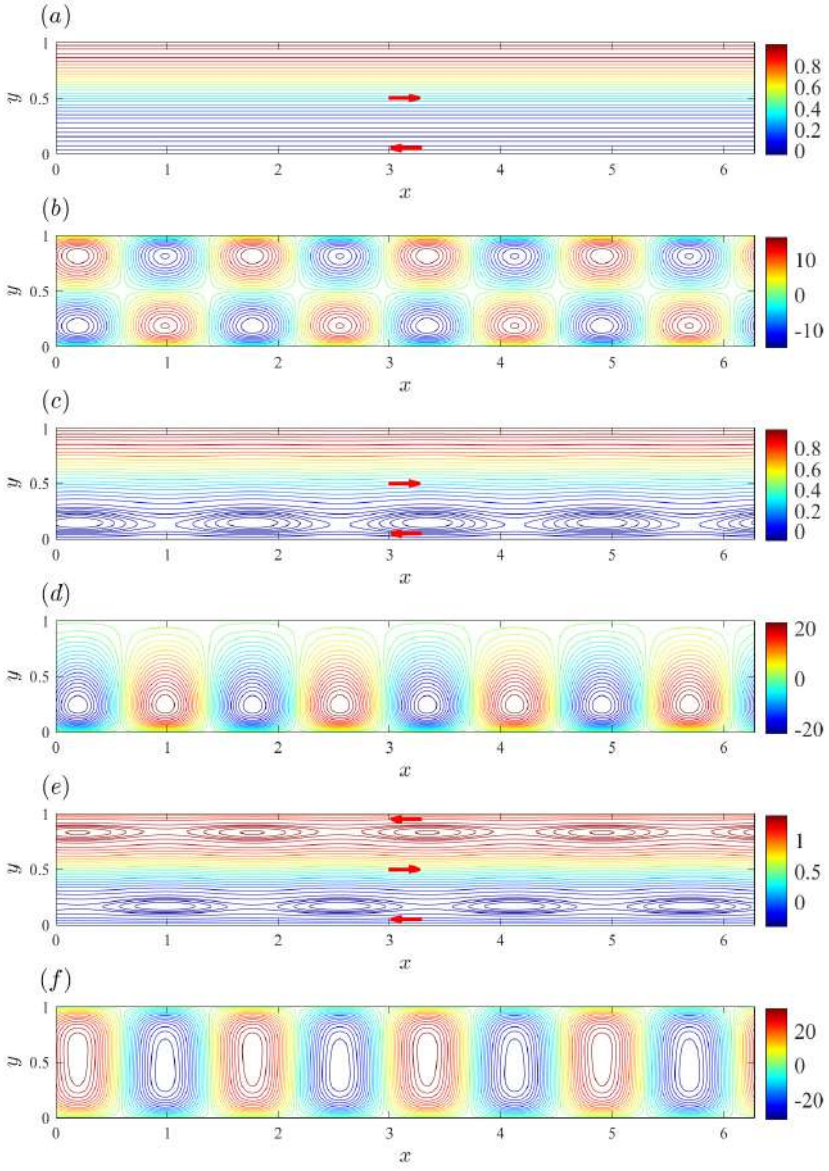

Figure 2: The typical streamlines of the channel Poiseuille flow with unique solution (a) or multiple solutions (b-f), wherein specific constant slip lengths are imposed on the both sides wall. (a) $\ell_0=-0.1$ and $\ell_d=0.1$; (b) $\ell_0=-0.1107$, $\ell_d=-0.1107$ and $A_n=E_n=3.3546$; (c) $\ell_0=-0.1236$, $\ell_d=0.1$ and $A_n=E_n=3.3546E-04$; (d) $\ell_0=-0.1236$, $\ell_d=0.1$ and $A_n=E_n=0.3355$; (e) $\ell_0=-0.1382$, $\ell_d=-0.1382$ and $A_n=E_n=3.3546E-03$; (f) $\ell_0=-0.1382$, $\ell_d=-0.1382$ and $A_n=E_n=3.3546$. The colour represents the value of the stream function. The red arrow indicates flow direction. $L=2\pi$, $d=1$ and $C=1$.

nel with the one-side slip and otherwise non-slip condition, i.e., $\ell_d=0$ and $V(x)=0$ in Eq. (2.1). Therefore, we use Eq. (2.2a) with Eq. (2.3) to represent its stream function.

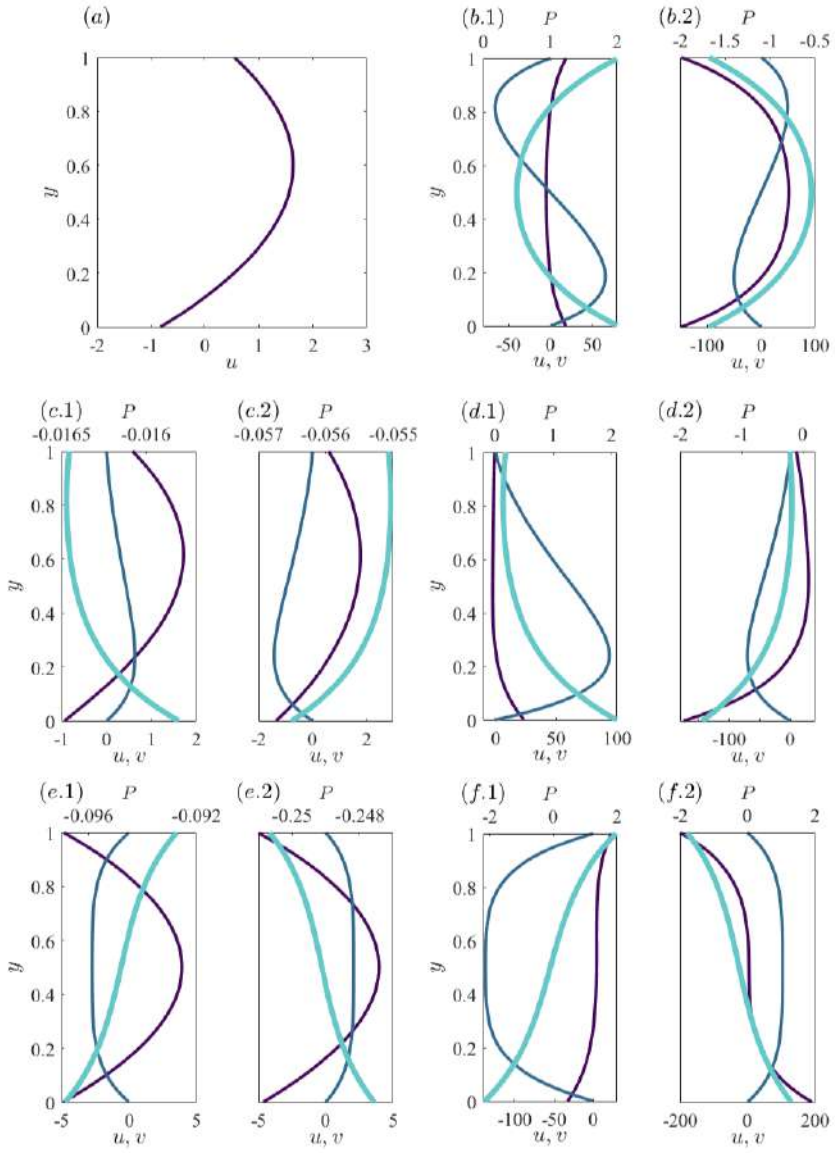

Figure 3: The corresponding velocity profiles and pressure profiles to Figs. 2(a)-(f). Profile position (a) $x=\pi$; (b.1) $x=1.3509$, (b.2) $x=3.5500$; (c.1) $x=1.0681$, (c.2) $x=3.5500$; (d.1) $x=1.3509$, (d.2) $x=3.5500$; (e.1) $x=1.3509$, (e.2)$x=3.5500$; (f.1) $x=1.3509$, (f.2) $x=3.5500$. The purple, blue, and cyan lines represent lateral velocity u, longitudinal velocity v, and pressure p respectively. In (a) the zero v and constant p are not shown. In (c,e) the 20 times v is presented.

Firstly, we substitute Eq. (2.3a) into boundary condition and obtain a linear algebraic equation set, the coefficient determinant of which can be given as $M_0=4d^3\ell_0+d^4$. Clearly, we have $M_0=0$ if ℓ_0 equals $-d/4$. Therefore, the equation set might have infinitely many

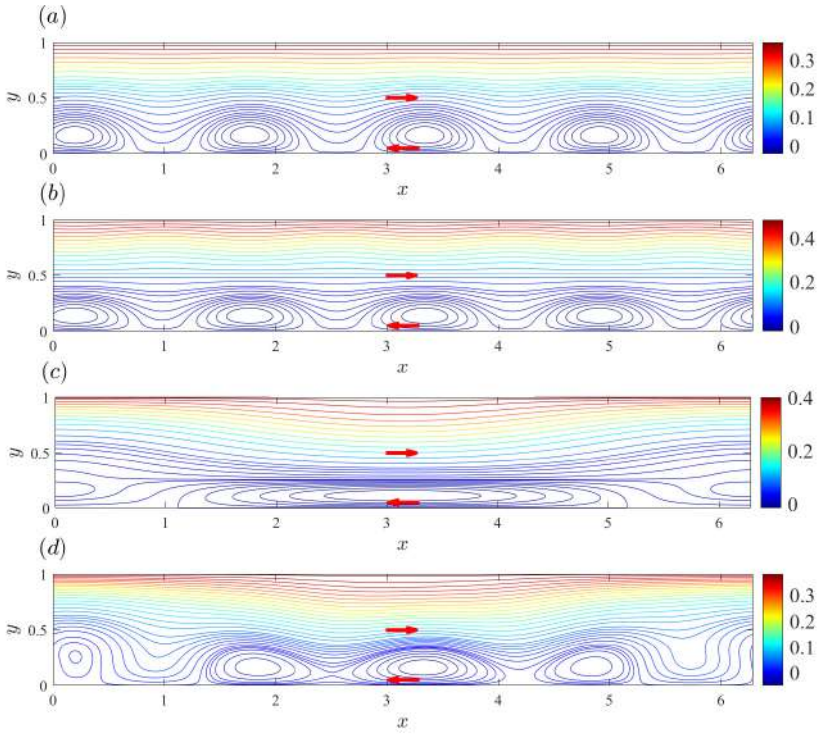

Figure 4: The typical streamlines of the channel Couette flow with multiple solutions (a-c) or unique solution (d), wherein specific constant slip lengths are imposed on the both sides wall. (a) $\ell_0=-0.1236$, $\ell_d=0.1$ and $A_n=E_n=3.3546E-04$; (b) $\ell_0=-0.1107$, $\ell_d=-0.1107$ and $A_n=E_n=3.3546E-03$; (c) $\ell_0=-0.1$ and $\ell_d=0.1$; (d) $\ell_0=-0.1236$, $\ell_d=0.1$ and $A_n=E_n=3.3546E-04$. With boundary driving condition (a,b) $V=1$ and (c,d) $V=1+\cos x$. The colour represents the value of the stream function. The red arrow indicates flow direction. $L=2\pi$ and $d=1$.

solutions when C equals zero or no solution when C does not equal zero. On the other hand, if ℓ_0 does not equal $-d/4$, the equation set has the unique solution.

As the same method above, for each $a_n(y)$ and $b_n(y)$, we can get a homogeneous linear system of equations following with the same with the same coefficient determinant M_n respectively. By calculation we conclude that, when ℓ_0 coincides with the following discrete values which depend on n, i.e.,

$$\ell_n=d\frac{1-\cosh(n_d)+n_d^2/2}{n_d\sinh(n_d)-n_d^2},\quad \frac{n_dL}{4\pi d}=1,2,\cdots, \tag{2.7}$$

the equations corresponding to $a_n(y)$ and $b_n(y)$ have infinitely many non-zero solutions, and the solutions for the other equations set are all zero. Conversely, if ℓ_0 does not takes any value presented in Eq. (2.7), then all the $a_n(y)$ and $b_n(y)$ are zero. For such case there is $\psi(x,y)=a_0(y)$ as the base flow, which is unique if $\ell\neq -d/4$ and multiple if $\ell=-d/4$ meanwhile $C=0$. For whatever case, the velocity profile of the base flow is a parabolic

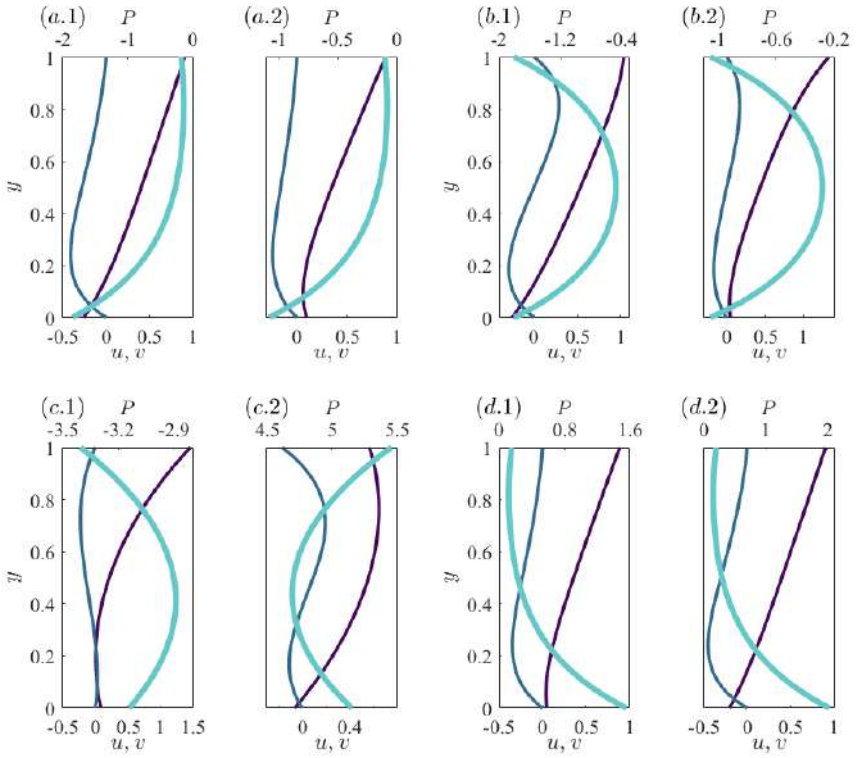

Figure 5: The corresponding velocity profiles and pressure profiles to Figs. 4(a)-(d). Profile position (a.1) $x=2.0316$, (a.2) $x=3.9898$; (b.1) $x=2.0316$, (b.2) $x=3.9898$; (c.1) $x=0.5760$, (c.2) $x=4.1783$; (d.1) $x=0.7749$, (d.2) $x=3.6547$. The purple, blue, and cyan lines represent lateral velocity u, longitudinal velocity v, and pressure p respectively. All v and p are enlarged by 5 and 10^3 times respectively.

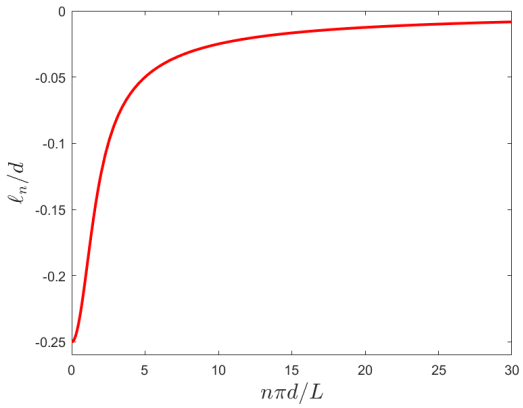

Figure 6: The normalized slip length ℓ_n/d leading to multiple solutions for Stokes flow imposed a constant slip length on the lower boundary of a two-dimensional channel, as a function of $n\pi d/L$.

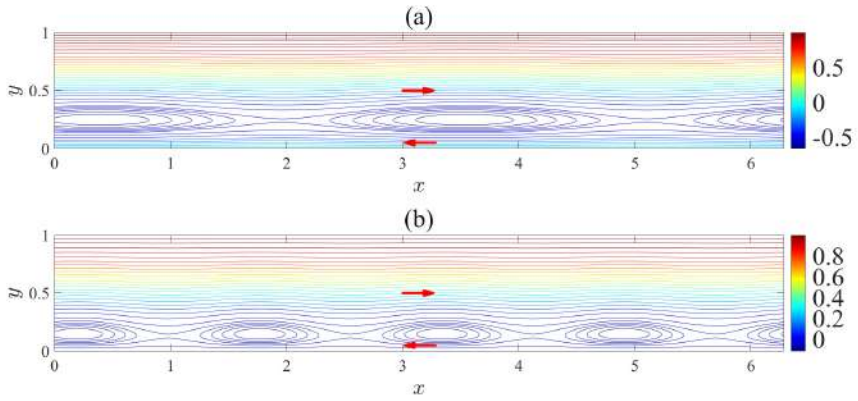

Figure 7: The typical streamlines of the channel flow with multiple solutions, where in a specific constant slip length is imposed on the lower wall. (a) $n=2$, $\ell_d=-0.1965$ and $A_n=E_n=0.0366$; (b) $n=4$, $\ell_d=-0.1229$ and $A_n=E_n=6.7093E-04$;. The colour represents the value of the stream function. The red arrow indicates flow direction. $L=2\pi$, $d=1$ and $C=1$.

as the Poiseuille flow, but there is a non-vanishing slip velocity on the lower plate where $y=0$.

Using the channel width d to normalize the slip length ℓ_n, and taking $n_d/4$ i.e., $n\pi d/L$ as the dimensionless variable, we plot the curve of the slip length corresponding to multiple solutions with respect to $n\pi d/L$ in Fig. 6. The curve tends to zero with the increase of n. At the same time, we find that the slip length ℓ_n leading to multiple solutions is always negative.

The case of multiple solution containing trigonometric function might be interesting, since the flow begin to display a variation along the streamwise, i.e., direction along the x-axis. To observe the flow pattern, we take different n and select one of the solutions to plot the streamline distribution as shown in Fig. 7. There are vortices at the lower boundary of flow field which is the same as the flow with the bilateral slip condition.

2.2 Flow in a plane annulus

We next consider the steady Stokes flow in a plane annulus domain ($a\leq r\leq b$). For such case the biharmonic equation can be solved by variable separation under cylindrical coordinates. It is easy to find that the stream function can be expressed as the following series form

$$\begin{aligned}\psi(r,\theta)=&Gr^2\ln r+Dr^2+E\ln r+F\\&+\left(A_1^{(1)}r^3+B_1^{(1)}r+C_1^{(1)}/r+D_1^{(1)}r\ln r\right)\cos\theta\\&+\left(A_1^{(2)}r^3+B_1^{(2)}r+C_1^{(2)}/r+D_1^{(2)}r\ln r\right)\sin\theta\end{aligned}$$

$$+\sum_{n=2}^{\infty}\Big[\Big(A_n^{(1)}r^{n+2}+B_n^{(1)}r^{-n+2}+C_n^{(1)}r^n+D_n^{(1)}r^{-n}\Big)\cos n\theta$$
$$+\Big(A_n^{(2)}r^{n+2}+B_n^{(2)}r^{-n+2}+C_n^{(2)}r^n+D_n^{(2)}r^{-n}\Big)\sin n\theta\Big], \tag{2.8}$$

with a variable rotation speed on the inner cylinder and constant slip length boundary conditions on the both side of cylinder

$$\begin{cases} \psi=0, & \dfrac{\partial\psi}{\partial r}=-\ell_b\dfrac{\partial^2\psi}{\partial r^2} & \text{at } r=b,\\ \psi=C, & \dfrac{\partial\psi}{\partial r}=\ell_a\dfrac{\partial^2\psi}{\partial r^2}-\Omega(\theta)a & \text{at } r=a, \end{cases} \tag{2.9}$$

where Ω is the angular velocity of inner boundary, which is expressed as

$$\Omega(\theta)=P_0+\sum_{n=1}^{\infty}[P_n\cos(n\theta)+Q_n\sin(n\theta)]$$

and P_0, P_n and Q_n are parameters of rotation velocity. All of the coefficients denoted by capital letters in Eq. (2.8) are constants to be determined by the boundary conditions, and the constant C expressing the flux in the boundary condition needs to be prescribed. Note that there is no flux through the boundaries, the stream function is single-valued and thus no term containing separate θ exists in the expression of ψ. Also, the proper flux condition C will result in a single value of flow field pressure, i.e., deducing $G=0$.

The terms irrelevant to θ in the stream function satisfy the equation set

$$\begin{cases} Ga^2\ln a+Da^2+E\ln a+F=C,\\ Gb^2\ln b+Db^2+E\ln b+F=0,\\ G[a(2\ln a+1)-\ell_a(2\ln a+3)]+D(2a-2\ell_a)+E(a+\ell_a)/a^2=-P_0a,\\ G[b(2\ln b+1)+\ell_b(2\ln b+3)]+D(2b+2\ell_b)+E(b-\ell_b)/b^2=0. \end{cases} \tag{2.10}$$

The condition for coefficient determinant M_0 of Eq. (2.10) to vanish is

$$\begin{aligned} &\frac{\ell_a}{a}\Big(\eta^4+2\eta^2-3-8\eta^2\ln\eta+4\eta^2\ln^2\eta\Big)+\frac{\ell_a\ell_b}{ab}\Big[3(\eta^2-1)^2+4\eta^2\ln^2\eta\Big]\\ &\quad+\frac{\ell_b}{b}\Big(3\eta^4-1-2\eta^2-8\eta^2\ln\eta-4\eta^2\ln^2\eta\Big)\\ =&4\eta^2\ln^2\eta-(\eta^2-1)^2, \end{aligned} \tag{2.11}$$

where $\eta\equiv b/a$, and therefore give the assertion for such slip lengths ℓ_a and ℓ_b that when $(C,P_0)=(0,0)$ the Eq. (2.10) has infinitely many solutions; and when $(C,P_0)\neq(0,0)$ the Eq. (2.10) might have no solution. Whether there is no solution or infinitely solutions depends on a complicated relation between (C,P_0), which will not be given here. For otherwise ℓ_a and ℓ_b, the Eq. (2.10) has unique solution.

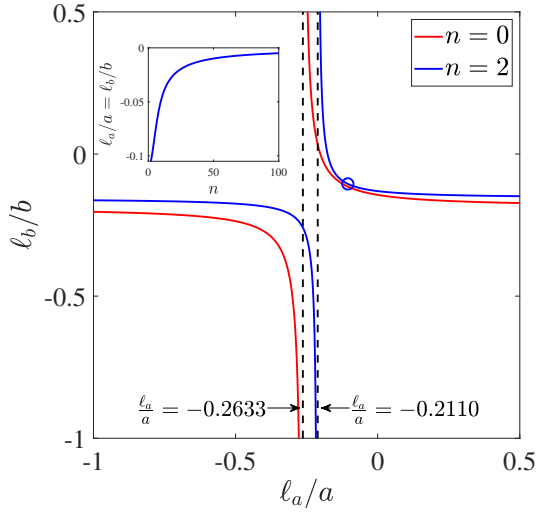

Figure 8: The (ℓ_a,ℓ_b) distribution leading to non-unique solution for Stokes flow imposed slip condition on the both sides boundary of a plane annulus. The plot does not serve as a further criterion for no solution or infinitely many solutions.

For those cases that the stream function containing θ-dependent terms, we discuss $n=1$ and $n\geq 2$ respectively. Substituting the boundary conditions and regulating its coefficient determinant $M_n=0$, we find two relationships for the slip lengths ℓ_a and ℓ_b as the following

$$\begin{aligned}
&\frac{\ell_a}{a}\left(2\eta^2-2-3\ln\eta-\eta^4\ln\eta\right)-\frac{\ell_a\ell_b}{ab}\left[(\eta^2-1)^2-3\ln\eta+3\eta^4\ln\eta\right]\\
&\quad+\frac{\ell_b}{b}\left(2\eta^4-2\eta^2-\ln\eta-3\eta^4\ln\eta\right)\\
&=\eta^4\ln\eta-\ln\eta-(\eta^2-1)^2, \qquad (2.12a)\\
&\frac{\ell_a}{a}\left[(\eta^{2n}-1)^2-2n(\eta^{4n}-1)+n^2(\eta^{2n+2}-3\eta^{2n-2}+2\eta^{2n})\right]\\
&\quad+\frac{\ell_a\ell_b}{ab}\left[(1-n^2)(\eta^{2n}-1)^2+3n^2(\eta^{2n+2}-1)(1-\eta^{2n-2})\right]\\
&\quad+\frac{\ell_b}{b}\left[n^2(3\eta^{2n+2}-\eta^{2n-2}-2\eta^{2n})-(\eta^{2n}-1)^2-2n(\eta^{4n}-1)\right]\\
&=(\eta^{2n}-1)^2-n^2(\eta^{n+1}-\eta^{n-1})^2, \qquad (2.12b)
\end{aligned}$$

corresponding to $n=1$ and $n\geq 2$, respectively. Obviously, if ℓ_a and ℓ_b satisfy Eq. (2.12a) or anyone or some of (2.12b) for finitely many numbers, the problem has non-unique solution. However, we find the further criterion for no solution or multiple solutions depends on (ℓ_a,ℓ_b,η) and n. The results are too trivial to be worthy of making a survey here, but we would rather like to do what follows.

We use radius a of inner cylinder to normalize ℓ_a and radius b to normalize ℓ_b, and plot the relation curve of the slip lengths ℓ_a and ℓ_b leading to multiple solutions or no solution with respect to n. Similar to the channel flow, it is shown in Fig. 8 that the curves of ℓ_0 and ℓ_d is similar to the channel, i.e., either both negative slip length or one positive and one negative (may be relatively small), which might lead the problem to have no solution.

If ℓ_a and ℓ_b do not meet all of the Eqs. (2.11)-(2.12b), then the problem has unique solution, irrelevant of the homogeneity of the boundary conditions. Under inhomogeneous boundary condition, the convergence of the series in Eq. (2.8) is similar to the case of channel flow, and the conclusion on classical solution is the same and shall not be presented here.

2.2.1 Two typical flows: Couette flow and Taylor-Dean flow

To see more clearly the influence of inhomogeneous conditions on the flow, we discuss two typical flow (i.e., Couette flow and Taylor-Dean flow) similarly to the channel as examples.

Firstly, when inner cylinder rotation speed is zero, i.e., $\Omega(x)=0$, the Taylor-Dean flow with the homogeneous slip boundary is driven by flux condition. The disappearance of boundary motion velocity results in the equation set for $a_n(y)$ and $b_n(y)$ homogenization, which has infinitely many solutions if ℓ_0 and ℓ_d have relation of the Eq. (2.12a) or (2.12b) and the terms for otherwise n are all zero. For $a_0(y)$, the vanishing boundary velocity has little effect, i.e., there is still no solution when ℓ_0 and ℓ_d satisfy relation of the Eq. (2.11).

On the other hand, when the value of pressure is single and the flow is driven by the boundary motion, we discuss the Couette flow with inner cylinder adjustable rotation speed. Clearly, for any n, if ℓ_0 and ℓ_d satisfy the Eq. (2.11), (2.12a) or (2.12b), when P_n or Q_n vanishes, the equation set for containing θ-dependent terms have multiple solutions, while if P_n and Q_n exist, the equation set might have no solution. On the contrary, when the Eqs. (2.11)-(2.12b) are all false, the Couette flow has the unique solution.

In channel flow, it is observed that the flow field has a large difference and the appearance of vortices due to different both sides slip boundary or partial slip boundary. To observe the flow situation in the plane annulus, we take $n=8$ with the appropriate slip length ℓ_a and ℓ_b relation and select one of the solutions to plot the streamline distribution and the corresponding velocity profiles and pressure profiles for Taylor-Dean flow and Couette flow. The results are shown in Figs. 9-12. We also see vortices in the flow field near the boundary with negative slip length, but the vortices may disappear when the boundary is driven by a relatively large speed. From the velocity profile (Figs. 12), it can be seen that the presence of velocity at the boundary reduces the radial velocity in the vicinity. In Figs. 11(d), (e), (f) of Couette flow, the boundary velocity is non-uniform, which results in that the flow field is no longer central symmetric, and vortices may be generated near boundary with the positive slip length.

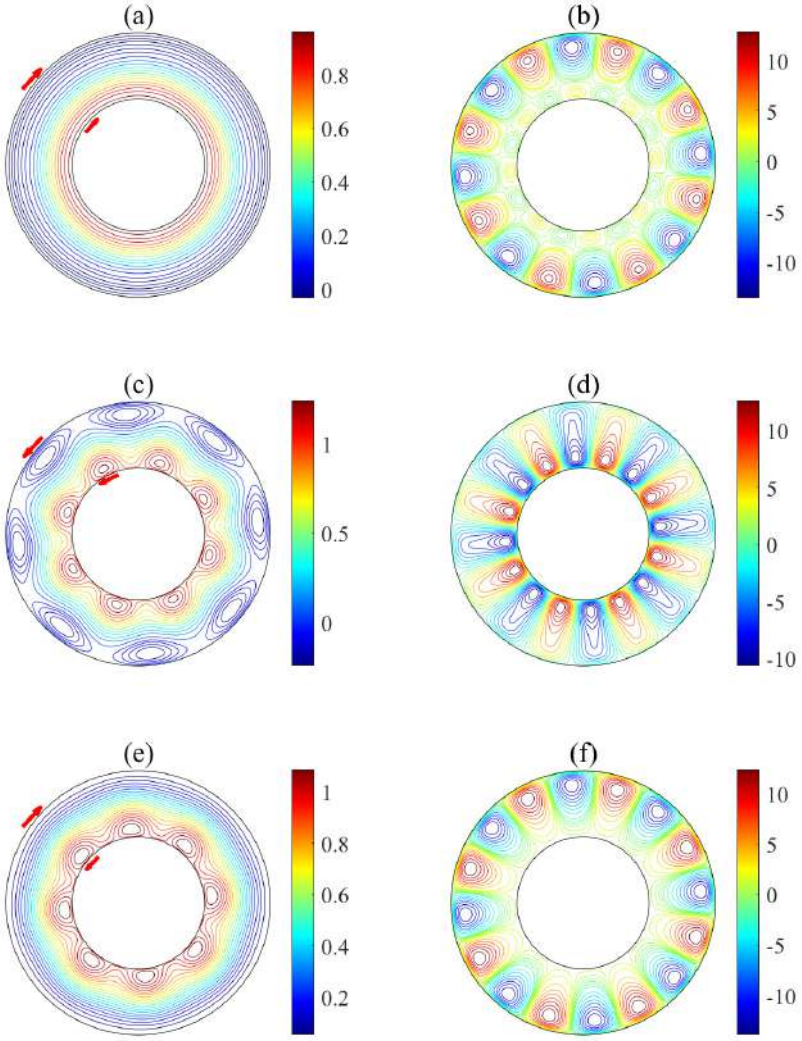

Figure 9: The typical streamlines of the plane annulus Taylor-Dean flow with unique solution (a) or multiple solutions (b-f), wherein specific constant slip lengths are imposed on the both sides wall. (a) $\ell_a=0.1$ and $\ell_b=-0.1$; (b) $\ell_a=-0.0582$, $\ell_b=-0.1164$ and $A_n^{(1)}=A_n^{(2)}=0.1172$; (c) $\ell_a=-0.0673$, $\ell_b=-0.1346$ and $A_n^{(1)}=A_n^{(2)}=7.8125E-04$; (d) $\ell_a=-0.0673$, $\ell_b=-0.1346$ and $A_n^{(1)}=A_n^{(2)}=0.0391$; (e) $\ell_a=-0.0666$, $\ell_b=-0.1$ and $A_n^{(1)}=A_n^{(2)}=3.9063E-05$; (f) $\ell_a=0.1$, $\ell_b=-0.1175$ and $A_n^{(1)}=A_n^{(2)}=0.1172$. The colour represents the value of the stream function. The red arrow indicates flow direction. $a=1$, $b=2$ and $C=1$.

2.2.2 Constant slip length on single-side boundary

Above, we study the Stokes flow in a plane annulus with inhomogeneous slip conditions on both inner and outer cylinders. We investigate the relation of bilateral slip lengths for multiple solutions and no solution of the stream function. If the slip length of one side

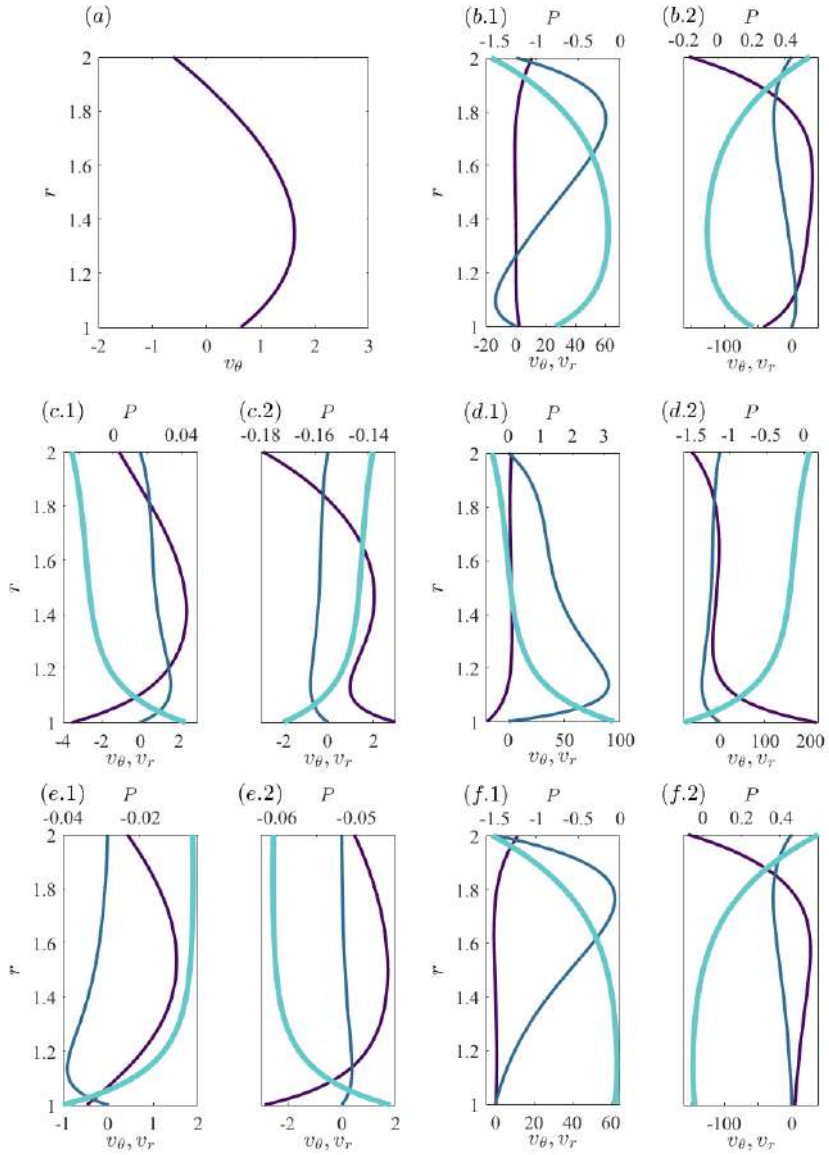

Figure 10: The corresponding velocity profiles and pressure profiles to Figs. 9(a)-(f). Profile position (a) $\theta=\pi$; (b.1) $\theta=0.3037$, (b.2) $\theta=3.1835$; (c.1) $\theta=0.3560$, (c.2) $\theta=3.1835$; (d.1) $\theta=0.3037$, (d.2) $\theta=3.1835$; (e.1) $\theta=0.3037$, (e.2) $\theta=3.1835$; (f.1) $\theta=0.3037$, (f.2) $\theta=3.1835$. The purple, blue, and cyan lines represent axial velocity v_θ, radial velocity v_r, and pressure p respectively. In (a) the zero v_r and constant p are not shown.

is zero, it will occur a more interesting situation, just like the channel. Therefore, in this part, we consider the steady Stokes flow in a plane annulus domain with an invariant rotation speed on the inner cylinder and a constant slip length boundary condition on the outer cylinder, i.e., $\ell_a=0$ and a constant Ω in Eq. (2.9).

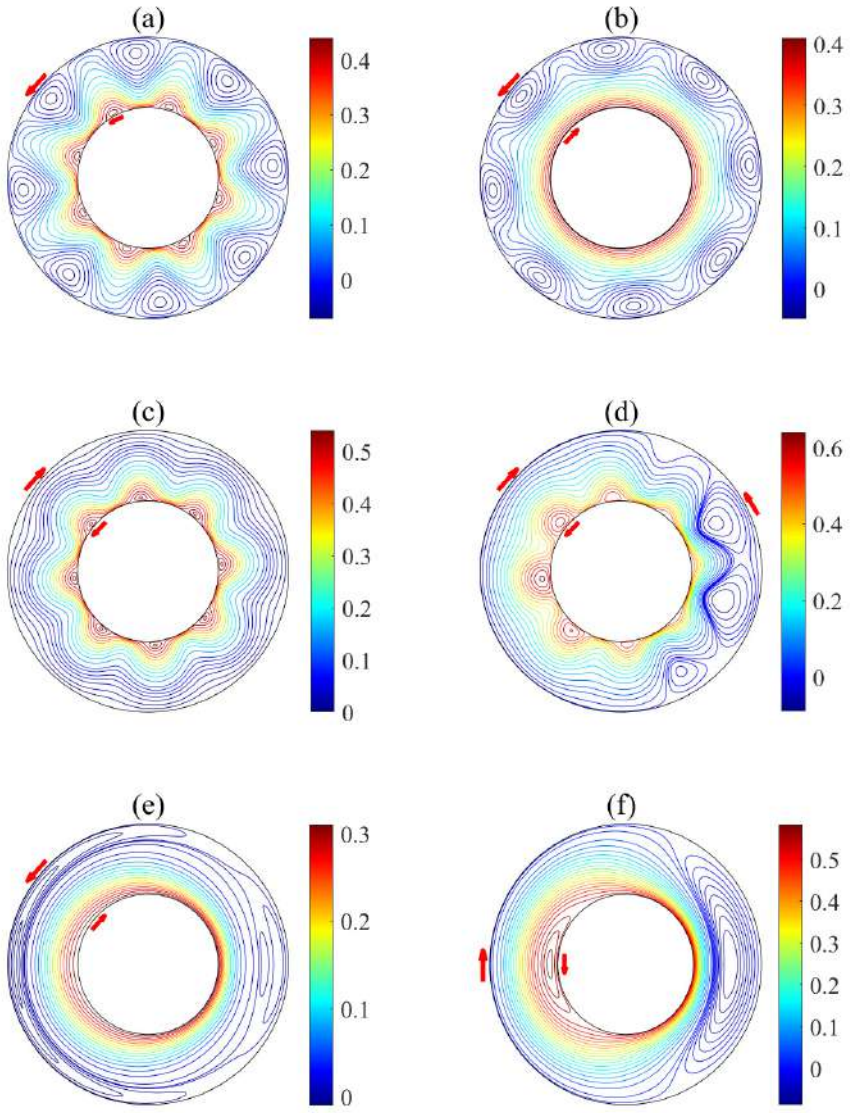

Figure 11: The typical streamlines of the plane annulus Couette flow with multiple solutions (a-d) or unique solution (e, f), wherein specific constant slip lengths are imposed on the both sides wall. (a) $\ell_a=-0.0673$, $\ell_b=-0.1346$ and $A_n^{(1)}=A_n^{(2)}=3.9063E-04$; (b) $\ell_a=-0.0582$, $\ell_b=-0.1164$ and $A_n^{(1)}=A_n^{(2)}=3.9063E-04$; (c) $\ell_a=-0.0666$, $\ell_b=-0.1$ and $A_n^{(1)}=A_n^{(2)}=3.9063E-05$; (d) $\ell_a=-0.0666$, $\ell_b=-0.1$ and $A_n^{(1)}=A_n^{(2)}=3.9063E-05$; (e) $\ell_a=0.1$ and $\ell_b=-0.1$; (f) $\ell_a=-0.1$ and $\ell_b=0.1$. With boundary driving condition (a,b,c) $\Omega=1$ and (d,e,f) $\Omega=1+\cos x$. The colour represents the value of the stream function. The red arrow indicates flow direction. $a=1$ and $b=2$.

Substituting Eq. (2.8) into boundary conditions, we consider the equation set of the terms independent on θ in the stream function. Let the value of coefficient determinant

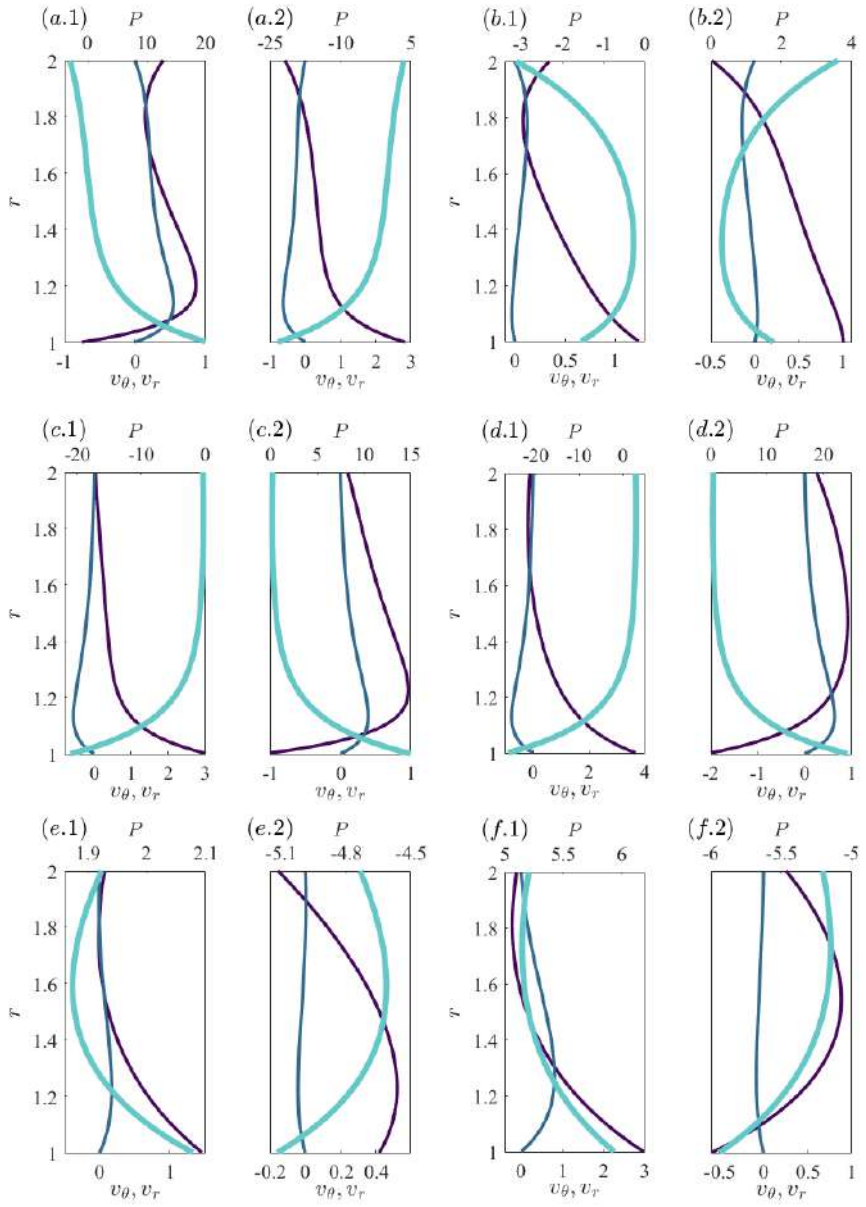

Figure 12: The corresponding velocity profiles and pressure profiles to Figs. 11(a)-(f). Profile position (a.1) $\theta=0.4084$, (a.2) $\theta=\pi$; (b.1) $\theta=0.4084$, (b.2) $\theta=\pi$; (c.1) $\theta=0.4084$, (c.2) $\theta=3.1835$; (d.1) $\theta=0.3560$, (d.2) $\theta=\pi$; (e.1) $\theta=0.3037$, (e.2)$\theta=3.9689$; (f.1) $\theta=0.4084$, (f.2) $\theta=3.5500$. The purple, blue, and cyan lines represent axial velocity v_θ, radial velocity v_r, and pressure p respectively. All p are enlarged by 10^3 times. In (e.1) and (f.1) the 10 times v_r is presented.

M_0 for above equation set be zero, we obtain a slip length

$$\ell_b = b\frac{1+\eta^4-2\eta^2-4\eta^2\ln^2\eta}{1-3\eta^4+2\eta^2+8\eta^2\ln\eta+4\eta^2\ln^2\eta}. \tag{2.13}$$

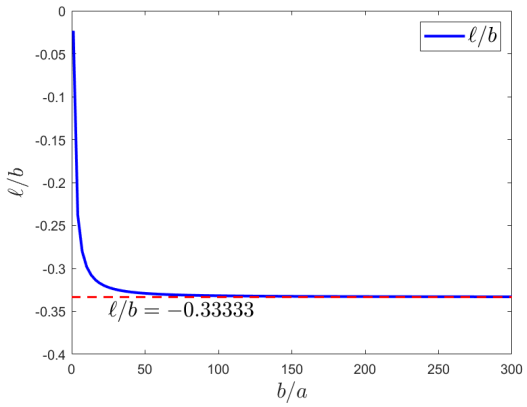

Figure 13: The relation between the normalized slip length leading to non-unique solution and the ratio of the outer and inner cylinder radius for Stokes flow in a plane annulus with a constant slip length imposed on the outer cylinder.

For such ℓ_b, when both of C and Ω equal zero the equation set has infinitely many solutions; when C or Ω does not equal zero the equation set might have no solution. If slip length ℓ_b does not satisfy Eq. (2.13), the equation set has unique solution no matter how the C and Ω take value. Fig. 13 shows the graph of Eq. (2.13). As η increases, that is, the annular cavity domain becomes wider, the value of ℓ_b/b tends to be $-1/3$.

Next, we discuss $n=1$ and $n\geq 2$ respectively. We regulate its coefficient determinant for each n to be zero, we obtain two expressions for the slip length as the following

$$\ell_1 = -b\frac{1+\eta^4-2\eta^2-\eta^4\ln\eta+\ln\eta}{2\eta^4-2\eta^2-\ln\eta-3\eta^4\ln\eta}, \tag{2.14a}$$

$$\ell_n = -b\frac{1+\eta^{4n}-\eta^{2n+2}n^2-\eta^{2n-2}n^2+2(n^2-1)\eta^{2n}}{1+\eta^{2n-2}n^2-3\eta^{2n+2}n^2-2n+(2n+1)\eta^{4n}+2(n^2-1)\eta^{2n}}, \tag{2.14b}$$

corresponding to $n=1$ and $n\geq 2$, respectively. If ℓ_b takes ℓ_1 or any ℓ_n $(n\geq 2)$, the linear equation set corresponding to the n-th term has infinitely many solutions, and the rest terms relevant to the otherwise n are all zero. If ℓ does not meet all the values ℓ_n $(n\geq 1)$, then all of the solution of all θ-dependent terms vanish. By analogy with channel flow, we use radius b of outer cylinder to normalize ℓ_n and plot the curve of the slip length leading to multiple solutions with respect to n under different η. Similar to the channel flow, it is shown in Fig. 14 that ℓ_ns are all negative and approach to zero asymptotically in a universal form as $n\to\infty$. In fact, the Eq. (2.14b) have an asymptotic expression $\ell_n \to -b/(2n)$ when $n\geq 10$, independent of η.

When $n\geq 1$, the results are the same as the previous situation. We take different n and select one of the solutions to plot the streamline distribution, see Figs. 15(a) and (b). Due to the symmetry of the domain, the configuration of the vortices also has a certain symmetry.

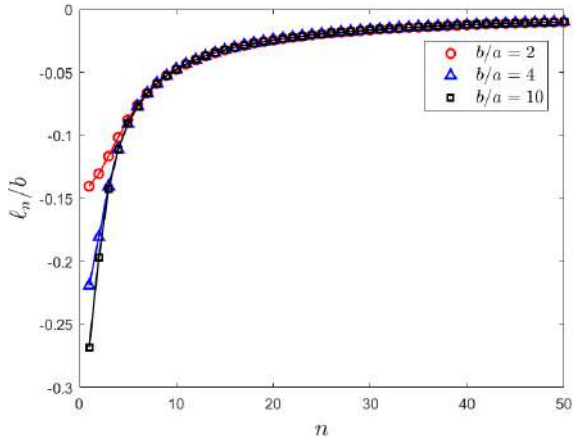

Figure 14: The normalized slip length ℓ_n/b leading to multiple solutions of Stokes flows imposed a constant slip length on the outer boundary of a plane annulus, as a function of n at different ratios b/a.

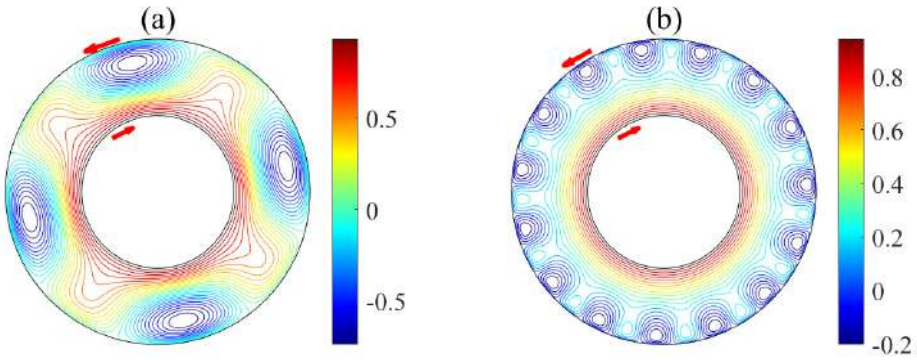

Figure 15: The streamlines as in Fig. 4 for (a) $n=4$, $\ell_b=-0.2032$ and $A_n^{(1)}=A_n^{(2)}=0.0625$; (b) $n=15$, $\ell_b=-0.0645$ and $A_n^{(1)}=A_n^{(2)}=3.0518E-05$;. The colour represents the value of the stream function. The red arrow indicates the flow direction. Here, $b=2$, $a=1$, $C=1$, and $\Omega=2$.

2.3 Flow in an axisymmetric circular pipe

We finally consider the axisymmetric Stokes flow in a z-periodic axisymmetric circular pipe ($r\leq a$, $0\leq z\leq L$), which is straight along the z-direction and whose radius is a. Using the cylindrical coordinate system, the equation that the axisymmetric Stokes stream function satisfies becomes $\Delta_s^2\psi=0$ where Δ_s is the Stokes operator. The general solution

of the Stokes stream function can be expressed as a series form with Bessel function [36]

$$\begin{aligned}\psi(r,z)=&A_0r^4+B_0r^2+E_0\\&+\sum_{n=1}^{\infty}\left[A_nrI_1\left(\frac{2n\pi r}{L}\right)+B_nr^2I_0\left(\frac{2n\pi r}{L}\right)\right]\cos\frac{2n\pi z}{L}\\&+\sum_{n=1}^{\infty}\left[C_nrI_1\left(\frac{2n\pi r}{L}\right)+D_nr^2I_0\left(\frac{2n\pi r}{L}\right)\right]\sin\frac{2n\pi z}{L},\end{aligned}\tag{2.15}$$

where I_1 and I_0 are modified Bessel function of the first kind, and A_n, B_n, C_n, D_n and E_0 are undetermined coefficients. The boundary conditions containing a slip on the pipe wall are

$$\begin{cases}\psi=0, & \dfrac{1}{r}\dfrac{\partial\psi}{\partial r}<\infty & \text{at } r=0,\\ \psi=C, & \dfrac{1}{r}\dfrac{\partial\psi}{\partial r}=-\ell\dfrac{\partial}{\partial r}\left(\dfrac{1}{r}\dfrac{\partial\psi}{\partial r}\right) & \text{at } r=a.\end{cases}\tag{2.16}$$

The terms independent of z in the stream function, i.e., the base flow, satisfy the equation set ($E_0=0$ can be set without changing the flow field)

$$\begin{cases}a^4A_0+a^2B_0=C,\\(4a^2+8\ell a)A_0+2B_0=0.\end{cases}\tag{2.17}$$

Similar to the first two flows we just discussed, the coefficient determinant of the above equation set can be calculated as $M_0=-8\ell a^3-2a^4$, and if $\ell=-a/4$, the value of the determinant will be zero. Therefore, when $C\neq0$ the Eq. (2.17) have no solution; when $C=0$ the Eq. (2.17) have infinitely many solutions; On the other hand, if $\ell\neq-a/4$, the Eq. (2.17) have unique solution.

For the Stokes stream function depending on z, each n corresponds to a set of linear equation. By calculating the coefficient determinant of the equation set, we obtain the slip length when the value of the determinant is zero, that is

$$\ell_n=-a\frac{I_0(2n^*)I_1(2n^*)-n^*I_0^2(2n^*)+n^*I_1^2(2n^*)}{2n^*I_1^2(2n^*)},\quad \frac{n^*L}{\pi a}=1,2,\cdots,\tag{2.18}$$

where $n^*\equiv n\pi a/L$. If ℓ satisfies Eq. (2.18), the n-th term in the stream function has infinitely many solutions and all of the rest terms for otherwise n vanish. For a general $\ell\notin\{\ell_n,\ n=1,2,\cdots\}$, however, all of the terms relevant to z in solution vanish. Using the radius a to normalize the slip length ℓ_n, and taking the n^* as a new independent variable, we plot the curve of the slip length leading to multiple solutions. See Fig. 16. Remarkably, it is shown that the curve for the circular pipe flow almost coincides as the one for the two-dimensional channel flow discussed previously.

We plot streamline graph for typical case of multiple solution in Fig. 17. It can be seen that the vortices in the three-dimensional axisymmetric circular pipe are somewhat different from those in the two-dimensional channel flow, indicating the influence of dimensionality.

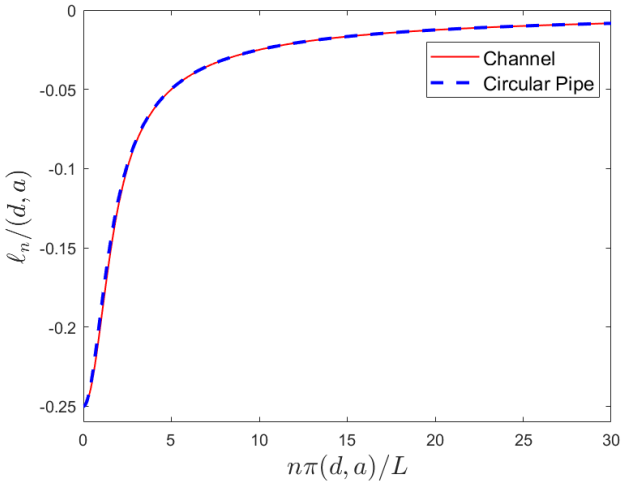

Figure 16: The normalized slip length leading to multiple solutions for the Stokes flow with a constant slip length on the wall in axisymmetric circular tube, as a function of n^*. The curve for the channel flow is presented again for comparison. For the channel flow, $n^* \equiv n\pi d/L$.

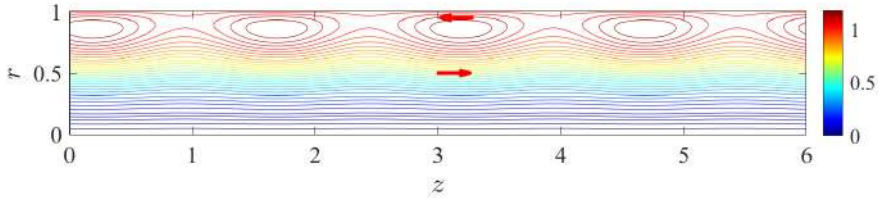

Figure 17: Typical streamlines of the axisymmetric circular pipe flow with multiple solutions. A specific constant slip length ℓ_n is imposed on the wall. The colour represents the value of the Stokes stream function. The red arrow indicates flow direction. Here, $n=4$, $\ell=-0.1143$, $A_n=C_n=0.0863$, $L=6$, $a=1$ and $C=1$.

3 Conclusions

In this work, we investigate Stokes flow imposed a Navier slip on boundary replacing the usual Dirichlet velocity condition [37]. The main concern is the well-posedness when the prescribed slip length is constant, particularly on the non-uniqueness of the solution as well as some interested physical of the flows. To simply the problem, three canonical domains of simple geometry are considered, including two-dimensional channel, plane annulus and axisymmetric circular pipe. For these domains the Stokes equations equipped the Navier slip condition on whole or certain nonpermeable boundary while the conventional non-slip or periodic condition keeps unchanged for otherwise boundary, can be solved by means of the series expansion for plane or Stokes stream function. It is found for all of the cases analysed that, while the problem is well-posed for almost all the prescribed value of slip length, remarkably the problem may have no solution or infinitely multiple solutions for a certain set of slip length at different boundaries. That is to say,

the uniqueness of the solution may not stand any longer under certain one positive and one negative or both negative slip lengths. For the Poiseuille flow with non-vanishing flux condition the case of no solution must be only related to the $n=0$ mode, i.e., the base flow case, while for the Couette flow with inhomogeneous boundary speed condition, the case of no solution may be related to all mode due to variable speed imposed on one boundary. Especially, for the plane channel flow and axisymmetric circular pipe flow with rigid boundary and slip on single-side boundary, the case of no solution can be along with a non-vanishing flux condition; and for plane annulus flow, the case of no solution must be along with a rotating inner cylinder with $\Omega(\theta)\neq 0$. However, there is not similar limitation for the cases of multiple solutions.

The set of the multiple solution corresponding to certain continuous function of slip length for each n consists of a simple base flow depending only on a single normal coordinate, i.e., y or r, or a vortical flow with an arbitrarily amplitude assigned and an appearance of neatly arranged vortices. The stream function of the vortical flow is the product of a comparatively complicated function of y or r and a single or several (at most two for channel flow) of trigonometric function with respect to streamwise coordinates which is x, θ or z for the three domains, respectively. Such structure is due to the linearity of the problem. As the magnitude of n increases, the wavenumber increases and the slip length relation changes so that there is a relatively small one positive and one negative slip length for multiple solution or no solution, and this material with small slip length exists realistically. In the case of multiple solutions, there are different vortices near the boundary. Therefore, the same slip length must correspond to different shear rate, which shows that the slip length is not just a single value function of the shear rate. In this work, we find that some slip boundary conditions lead to multiple solutions or no solution of the problem, which indicates that the flow fields with different boundary velocities and boundary shear rates may have the same boundary slip length, and no matter how the flow field changes, the slip length corresponding to the no solution case can not be realized, respectively. These observations imply a fact that the slip length on solid boundary is not only a physical parameter to character specific material as solid-fluid interface, but also a flow field parameter.

In present literatures, the negative slip length is mathematically meaningful [32, 33] and physically defined as the thickness of the immobile fluid layer in the vicinity of a solid surface [5, 11, 12, 14, 15, 38]. The negative slip length indicates that the attractive force between solid and fluid is so large that the fluid is adsorbed onto the solid walls. However, some simulation show that liquid water can still slip even if the solid wall is hydrophilic material [12, 39, 40]. In this work, it can be seen from Figs. 2, 4, 7, 9, 11, 15 and 17 that there is reverse flow near and on the negative slip boundary. The reverse velocity caused by negative slip is actually equivalent to the non-slip condition of a specific moving wall. Overall, the negative slip length corresponding to no solution and multiple solutions might be of some significance for the study of micro-nano scale flows and their managements.

From a viewpoint of mathematics, this paper actually suggests a study on the well-

posedness for a high-order Robin problem for planar biharmonic equation, as well as an ordinary Robin problem for three-dimensional Stokes equations or even the nonlinear Navier-Stokes equations. To our best knowledge, the study on possible non-uniqueness of the solution is still open under general cases. Therefore, further researches are desired in future.

Appendix

A Laplace equation in periodic channel under an inhomogeneous Robin boundary condition

Let us consider the Laplace equation in a two-dimensional x-periodic channel domain $(0\leq x\leq L,\ 0\leq y\leq d)$

$$\nabla^2 v=0, \tag{A.1}$$

with the following inhomogeneous Robin conditions

$$\begin{cases} v=t_0\dfrac{\partial v}{\partial y} & \text{at } y=0, \\ v=-t_d\dfrac{\partial v}{\partial y}+V(x) & \text{at } y=d, \end{cases} \tag{A.2}$$

where t_0 and t_d are constants, and $V(x)$ is a prescribed L-periodic function expressed by a Fourier series as

$$V(x)=V_0+\sum_{n=1}^{\infty}[V_n\cos(2\pi nx/L)+W_n\sin(2\pi nx/L)].$$

By separating variables method, the general solution of the Laplace equation in channel can be obtained as

$$v(x,y)=A_0y+B_0+\sum_{n=1}^{\infty}\left[a_n(y)\cos\left(\frac{2\pi nx}{L}\right)+b_n(y)\sin\left(\frac{2\pi nx}{L}\right)\right], \tag{A.3}$$

where

$$a_n(y)=A_ne^{2\pi ny/L}+B_ne^{-2\pi ny/L},\quad b_n(y)=C_ne^{2\pi ny/L}+D_ne^{-2\pi ny/L},$$

and those constants denoted by capital letters are undetermined coefficients depending on the boundary conditions.

The coefficients A_0 and B_0 satisfy the equation set

$$\begin{cases} t_0A_0-B_0=0, \\ (t_d+d)A_0+B_0=V_0. \end{cases} \tag{A.4}$$

The value of the coefficient determinant of Eq. (A.4) is t_0+t_d+d. If $t_0+t_d\neq -d$, the Eq. (A.4) have unique solution. Otherwise, the Eq. (A.4) might have infinitely many solutions when $V_0=0$ or no solution when $V_0\neq 0$.

Subsequently, we substitute the expressions of $a_n(y)$ and $b_n(y)$ into Eq. (A.2) and calculate the value of the coefficient determinant of the linear equation set for solving A_n and B_n. The condition to make the value vanish reads

$$\frac{t_0+t_d}{d}n_L\cosh(n_L)+\left(\frac{t_0t_d}{d^2}n_L^2+1\right)\sinh(n_L)=0,\quad \frac{n_LL}{2\pi d}=1,2,\cdots, \tag{A.5}$$

where $n_L=2\pi dn/L$. The linear equation sets to determine (A_n,B_n) and (C_n,D_n) as coefficients have inhomogeneous terms V_n and W_n respectively. When t_0 and t_d do not meet Eq. (A.5) for any natural number n, the coefficients equation sets have unique solution. This is the case when both t_0 and t_d are non-negative. Otherwise, it is possible that Eq. (A.5) can be satisfied under appropriate (t_0,t_d,n) and hence the coefficients equation sets will have infinitely many solutions or no solution, depending on whether the V_n and W_n vanish or not. Moreover, it is interesting to notice that there may indeed be left two distinct n-terms in the infinite series expression Eq. (A.3) in the case of multiple solutions, for which usually only one n-term is left in the series.

Based on the above analysis, we demonstrate the following result: for the Laplace equation in periodic channels under the Robin condition with constant slip lengths, there are possibly infinitely many solutions or no solution when two slip lengths on the boundaries have opposite signs, or both slip lengths are negative.

B Convergence and differentiability of the stream function series

We take the cosine series of the stream function in channel (Eq. (2.2a)) as an example to prove the uniform convergence of the series and its derivatives at appropriate high orders. Here, we assume that $V(x)$ (Eq. (2.2b)) is a function up to m-order differentiable with a period of L, and the m-th order derivative function of $V(x)$ is piece-wise monotonic and continuous in $[0,L]$. This condition means that the Fourier series of the $V^{(m)}(x)$ is point-wise convergent.

First, recall

$$a_n(y)=(A_n+B_ny)e^{2\pi ny/L}+(C_n+D_ny)e^{-2\pi ny/L}$$

and the following boundary condition (Eq. (2.1))

$$\begin{cases} a_n(0)=0, \\ a_n'(0)=\ell_0a_n''(0), \\ a_n(d)=0, \\ a_n'(d)=-\ell_da_n''(d)+V_n. \end{cases} \tag{B.1}$$

The coefficient determinant of the linear algebraic equations to determine (A_n,B_n,C_n,D_n) can be calculated as

$$\begin{aligned}M_n=&\frac{4n\pi}{L}(\ell_0+\ell_d)\left(e^{4\pi nd/L}-e^{-4\pi nd/L}\right)-\frac{32n^2\pi^2}{L^2}(\ell_0\ell_d+d\ell_0+d\ell_d)\\&+\left(1+\frac{16\ell_0\ell_d n^2\pi^2}{L^2}\right)\left(e^{4\pi nd/L}+e^{-4\pi nd/L}\right)-\frac{16d^2n^2\pi^2}{L^2}-2.\end{aligned}\tag{B.2}$$

In Appendix C, we show that there are at most only one or two n-zeros as natural numbers to make $M_n=0$ for a set of given (ℓ_0,ℓ_d). Therefore, the infinite series in Eq. (2.2a) will become finite sums of smooth functions if $M_n=0$. For such case the differentiability of the stream function is trivial. Thus we will concentrate to the case of $M_n\neq 0$. For this case there is the unique solution

$$\begin{cases}A_n=-\dfrac{V_nd\left(Le^{4\pi nd/L}-L+4\pi n\ell_0+4\pi n\ell_0e^{4\pi nd/L}\right)}{e^{2\pi nd/L}LM_n},\\[2ex]B_n=-\dfrac{V_n\left(L-\ Le^{4\pi nd/L}+4\pi nd+4\pi n\ell_0-4\pi n\ell_0e^{4\pi nd/L}\right)}{e^{2\pi nd/L}LM_n},\\[2ex]C_n=\dfrac{V_nd\left(Le^{4\pi nd/L}-L+4\pi n\ell_0+4\pi n\ell_0e^{4\pi nd/L}\right)}{e^{2\pi nd/L}LM_n},\\[2ex]D_n=\dfrac{V_n\left(L-Le^{4\pi nd/L}-4\pi n\ell_0+4\pi nde^{4\pi nd/L}+4\pi n\ell_0e^{4\pi nd/L}\right)}{e^{2\pi nd/L}LM_n}.\end{cases}\tag{B.3}$$

Subsequently, we deduce the q-th order derivative of Eq. (2.3b) with respect to y by Leibniz rule and substitute Eq. (B.3) into the expression. This yields

$$\frac{d^qa_n(y)}{dy^q}=-\left(\frac{2n\pi}{L}\right)^{q-1}\frac{D_q}{LM_n}V_n,\tag{B.4}$$

where

$$\begin{aligned}D_q\equiv&I_fe^{2\pi n(y-d)/L}+(-1)^qI_ge^{-2\pi n(y+d)/L},\\I_f\equiv&e^{4\pi nd/L}\left(-qL-4\pi nq\ell_0+2\pi n(d-y)+\frac{8\pi^2n^2(d-y)\ell_0}{L}\right)\\&+\left(4\pi nq(d+\ell_0)+qL-2\pi n(d-y)+\frac{8\pi^2n^2(d\ell_0+\ell_0y+yd)}{L}\right),\\I_g\equiv&e^{4\pi nd/L}\left(4\pi nq(d+\ell_0)-qL-2\pi n(d-y)-\frac{8\pi^2n^2(d\ell_0+\ell_0y+yd)}{L}\right)\\&+\left(qL-4\pi nq\ell_0+2\pi n(d-y)-\frac{8\pi^2n^2(d-y)\ell_0}{L}\right).\end{aligned}$$

It is expected that the derivative function of the series can be obtained by differentiating the series term by term. In other words, we need to prove that

$$\frac{\partial^{p+q}}{\partial x^p \partial y^q}\left(\sum_{n=1}^{\infty} a_n(y)\cos\left(\frac{2\pi n x}{L}\right)\right)=\sum_{n=1}^{\infty}\frac{d^q a_n(y)}{dy^q}\left(\frac{2\pi n}{L}\right)^p(-1)^{[\frac{p}{2}]}\begin{pmatrix}\cos\\ \sin\end{pmatrix}\left(\frac{2\pi n x}{L}\right), \quad \text{(B.5)}$$

where in the r.h.s of Eq. (B.5) the cosine is taken when p is even and the sine is taken when p is odd. For simplicity we shall term the series in the r.h.s of Eq. (B.5) as the *primary series*. The uniform convergence of the primary series for $p+q=0,1,2,\cdots,m$ in the domain $\{(x,y)\in[0,L]\times[0,d]\}$ will be proved below. This confirms that the series is derivable term by term no matter with respect to y or x. Hence, the stream function represented by the infinite series is indeed the desired classical solution of the bi-harmonic equation under the boundary conditions with constant slip lengths. Moreover, we prove that the stream function is actually C^∞ with respect to $y\in[0,d)$ and $x\in[0,L]$.

Since $a_n(d)\equiv 0$, the series itself converge to zero to produce a smooth function $\psi(x,d)\equiv C$. Thus from now on when discussing the convergence of the series at $y=d$, we will assume $q\neq 0$ unless noted otherwise.

According to the distribution of slip lengths, there are several cases for discussion.

Case 1. $\ell_0\neq 0$ and $\ell_d=0$.

Obviously, $\exists N_1(L,d,\ell_0)\in\mathbb{N}$, s.t. $\forall n>N_1$, in the asymptotic sense of approximation at any precision, there is

$$\begin{aligned}\frac{d^q a_n(y)}{dy^q}\sim-\left(\frac{2\pi n}{L}\right)^{q-1}V_n\Bigg(&e^{-\frac{2\pi n}{L}(d-y)}\left(-\frac{qL}{4\pi n\ell_0}-q+\frac{d-y}{2\ell_0}+\frac{2\pi n(d-y)}{L}\right)\\&+e^{-\frac{2\pi n}{L}(3d-y)}\left(\frac{q(d+\ell_0)}{\ell_0}+\frac{qL}{4\pi n\ell_0}-\frac{d-y}{2\ell_0}+\frac{2\pi n(d\ell_0+\ell_0 y+yd)}{L\ell_0}\right)\\&+(-1)^q e^{-\frac{2\pi n}{L}(d+y)}\left(\frac{q(d+\ell_0)}{\ell_0}-\frac{qL}{4\pi n\ell_0}-\frac{d-y}{2\ell_0}-\frac{2\pi n(d\ell_0+\ell_0 y+yd)}{L\ell_0}\right)\\&+(-1)^q e^{-\frac{2\pi n}{L}(3d+y)}\left(-q+\frac{qL}{4\pi n\ell_0}+\frac{d-y}{2\ell_0}-\frac{2\pi n(d-y)}{L}\right)\Bigg).\end{aligned} \quad \text{(B.6)}$$

On the upper boundary, i.e., $y=d$, Eq. (B.6) yields a clearer result. That is

$$\frac{d^q a_n(y)}{dy^q}\sim-\left(\frac{2\pi n}{L}\right)^{q-1}qV_n. \quad \text{(B.7)}$$

Due to $V(x)\in C^m([0,L])$ and its periodicity, the Fourier series

$$\sum_{n=1}^{\infty}\left(\frac{2\pi n}{L}\right)^{p+q-1}V_n\begin{pmatrix}\cos\\ \sin\end{pmatrix}\left(\frac{2\pi n x}{L}\right), \quad \text{(B.8)}$$

are uniformly convergent series for x when $p+q-1\leq m-1$, and are point-wise convergent up to $p+q-1=m$. Thus, for $x\in[0,L]$ and $y=d$, the primary series are uniformly convergent

for $0\leq p+q\leq m$ and point-wise convergent for $0\leq p+q\leq m+1$. In the last two inequalities $q=0$ is allowed.

On the other hand, we consider the case of $y\in[0,d)$. A further asymptotic analysis to Eq. (B.6) implies that, for any positive δ satisfying $0<\delta<d$ and $\forall y\in[0,d-\delta]$ there will be

$$\left|\frac{d^q a_n(y)}{dy^q}\right|\sim\left|\left(\frac{2\pi n}{L}\right)^q V_n e^{-\frac{2\pi n}{L}(d-y)}(d-y)\right|\leq\left(\frac{2\pi n}{L}\right)^q|V_n|e^{-\frac{2\pi n}{L}\delta}d. \tag{B.9}$$

It is evident that the primary series has a uniform majorant series that is absolutely convergent for each $x\in[0,L]$ and $y\in[0,d-\delta]$. This guarantees the uniform convergence of the primary series for any nonnegative integer p,q for $(x,y)\in[0,L]\times[0,d-\delta]$. Since δ can be arbitrary small, the conclusion holds for $(x,y)\in[0,L]\times[0,d)$.

Case 2: $\ell_0=0$ and $\ell_d\neq 0$.

Case 3: $\ell_0=\ell_d=0$.

Case 4: $\ell_0\ell_d\neq 0$.

The analyses for these cases are completely similar to Case 1. The different variants of the asymptotic expression of $d^q a_n(y)/dy^q$ make no difference on the conclusion.

For the sine part of the stream function, obviously the analysis is the same other than the V_n is replaced by the W_n. And thus the convergence property of the alike primary series is the same.

In summary, we have proved that the series in Eq. (2.2a) and its form differentiated term by term with respect to x and y are uniformly convergent up to the highest order of the differentiation of the velocity function $V(x)$ on the line $y=d$ and is uniformly convergent up to arbitrary order for $(x,y)\in[0,L]\times[0,d)$. On the line of $y=d$, the point-wise convergence of the derivative series is up to the $(m+1)$-th order. These properties of convergence indicate that the stream function is C^∞ with respect to x and y in the interior of the channel and is of one order higher smoothness than the $V(x)$ on the upper boundary of the channel.

In other words, actually we have proved the existence of classical solution for the Stokes problem imposed a constant Navier slip length on the lower and upper walls of a periodic channel. For other domains studied in this paper, it is believed the stream functions presented by the infinite series are also the classical solution. To avoid over redundancy, however, we shall not discuss the problem any longer in this paper.

C The zeros of the determinant M_n

For the channel flow, when $a_n(y)$ satisfies homogeneous boundary conditions

$$\begin{cases} a_n(0)=0, \\ a_n'(0)=\ell_0 a_n''(0), \\ a_n(d)=0, \\ a_n'(d)=-\ell_d a_n''(d), \end{cases} \tag{C.1}$$

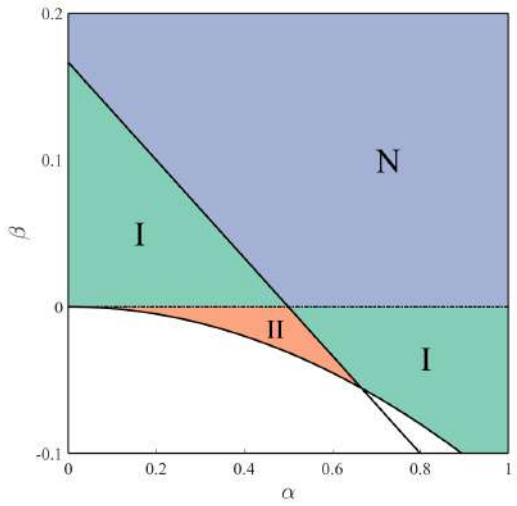

Figure 18: The phase diagrams about the distribution of zeros of $M(x)$ (i.e., M_{n_d}). Region N indicates that $M(x)$ has no zero point. Region I indicates that $M(x)$ has a unique zero point, while Region II indicates that $M(x)$ has two zero points. The slant line is $2\alpha+6\beta=1$, and the curve is the parabolic $\alpha^2+8\beta=0$. By Schwarz inequality, the region lower than the parabolic is unrealizable since the slip lengths ℓ_0 and ℓ_d are real numbers. Region I and N with $\beta>0$ can be extended to the whole upper half plane, while the unshown region of $\alpha<0$ and $\beta<0$ is also of null zero. The borderlines of adjacent regions belong to the Region of fewer zero point.

the coefficient determinant M_n presented in Eq. (B.2) can be transformed into

$$M_{n_d}=2n_d\frac{\ell_0+\ell_d}{d}[\sinh(n_d)-n_d]-2n_d^2\frac{\ell_0\ell_d}{d^2}[1-\cosh(n_d)]+2\cosh(n_d)-n_d^2-2, \tag{C.2}$$

where $n_d\equiv 4\pi dn/L$. When $M_{n_d}=0$, the linear equation set to determine the coefficients (A_n,B_n,C_n,D_n) has nonzero solutions. To answer the question that how many distinct n could make M_n vanish at the same time and the relevant Fourier modes would be therefore remained in the series in Eq. (2.2a), we need to investigate the distribution of the zeros of M_{n_d} in detail. On this purpose, by rewriting Eq. (C.2) we consider the function defined on $x\in(0,\infty)$

$$M(x)=\alpha f(x)+\beta g(x)-h(x), \tag{C.3}$$

where

$$\alpha=-2(\ell_0+\ell_d)/d,\quad \beta=-2(\ell_0\ell_d)/d^2,\qquad f(x)\equiv x(\sinh x-x),$$
$$g(x)\equiv x^2(\cosh x-1),\qquad h(x)\equiv 2(\cosh x-1)-x^2.$$

Obviously,

$$\lim_{x\to 0}\frac{f(x)}{g(x)}=\frac{1}{3},\quad \lim_{x\to 0}\frac{h(x)}{g(x)}=\frac{1}{6},\quad f(x)>2h(x)>0,\quad g(x)>3f(x)>0. \tag{C.4}$$

After classification discussion, the phase diagrams about the distribution of zero-points of $M(x)$ with respect to α and β is shown in Fig. 18. It can be seen that the distribution region of the zeros of $M(x)$ is divided into three: no zero point, one zero and two zeros.

It should be emphasized that the zero-point of $M(x)$ Region I and II just provide a necessary but not sufficient condition for the existence of the possible zeros of M_n. For a given (α,β) falling into Region I, the sole zero of M_n appear only when the zero x_0 of $M(x)$ satisfies that $x_0L/(4\pi d)$ is a natural number. Similarly, for a given (α,β) falling into Region II, the two zeros (x_1,x_2) of $M(x)$ become the zeros of M_n only when both $x_1L/(4\pi d)$ and $x_2L/(4\pi d)$ are natural numbers. In fact, only those (α,β) are meaningful that make two zeros generate a rational ratio. It is found that the ratio may be arbitrarily great when β approximates to 0^- inside Region II in Fig. 18. This implies that the wave numbers of the two modes in the series in Eq. (2.2a) consisting the nontrivial x-relevant solution of the stream function can be dramatically distinct. This is possibly an interesting phenomenon worthy of further study in the future.

Acknowledgements

The authors would like to thank the anonymous reviewers for their valuable suggestions. This work is supported by the National Natural Science Foundation of China Project (No. 91752203).

References

[1] D. Bernoulli, *Specimen theoriae novae de mensura sortis,* Comment. Acad. Sci. Imper. Petro., 5 (1738), pp. 175–192.
[2] C. Navier, *Mémoire sur les lois du mouvement des fluides,* Mémo. Acad. Roy. Sci. Inst. France, 6 (1823), pp. 389–440.
[3] P. Debye and R. L. Cleland, *Flow of liquid hydrocarbons in porous vycor,* J. Appl. Phys., 30 (1959), pp. 843–849.
[4] J. P. Rothstein, *Slip on superhydrophobic surfaces,* Annu. Rev. Fluid Mech., 42 (2009), pp. 89–109.
[5] R. Wang, J. Chai, B. Luo, X. Liu, J. Zhang, M. Wu, M. Wei and Z. Ma, *A review on slip boundary conditions at the nanoscale: recent development and applications,* Beilstein J. Nanotechnol., 12 (2021), pp. 1237–1251.
[6] S. Prakash, M. Pinti and B. Bhushan, *Theory, fabrication and applications of microfluidic and nanofluidic biosensors,* Phil. Trans. Roy. Soc. A-Math. Phys. Eng. Sci, 370 (2012), pp. 2269–2303.
[7] B. J. Kirby, Micro- and Nanoscale Fluid Mechanics: Transport in Microfluidic Devices, Cambridge University Press, Cambridge, 2010.
[8] G. Karniadakis, A. Beskok and N. Aluru, Microflows and Nanoflows: Fundamentals and Simulation, Springer Science, 2006.
[9] P. Joseph and P. Tabeling, *Direct measurement of the apparent slip length,* Phys. Rev. E, 71 (2005), 035303.

[10] D. C. Tretheway and C. D. Meinhart, *Apparent fluid slip at hydrophobic microchannel walls,* Phys. Fluids, 14(3) (2002), pp. L9–L12.
[11] J. Zhang, H. Q. Song, W. Y. Zhu and J. L. Wang, *Liquid transport through nanoscale porous media with strong wettability,* Trans. Porous Media, 140 (2021), pp. 697–711.
[12] J. Hyväluoma and J. Harting, *Slip flow over structured surfaces with entrapped microbubbles,* Phys. Rev. Lett, 100 (2008), 246001.
[13] H. Tian, J. Zhang, E. Wang, Z. Yao and N. Jiang, *Experimental investigation on drag reduction in turbulent boundary layer over superhydrophobic surface by TRPIV,* Theo. Appl. Mech. Lett, 5 (2015), pp. 45–49.
[14] B. Pottier, C. Frétigny and L. Talini, *Boundary condition in liquid thin films revealed through the thermal fluctuations of their free surfaces,* Phys. Rev. Lett., 114 (2015), 227801.
[15] S. Gruener, D. Wallacher, S. Greulich, M. Busch and P. Huber, *Hydraulic transport across hydrophilic and hydrophobic nanopores: Flow experiments with water and n-hexane,* Phys. Rev. E, 93 (2016), 013102.
[16] J. Ou, B. Perot and J. P. Rothstein, *Laminar drag reduction in microchannels using ultrahydrophobic surfaces,* Phys. Fluids, 16 (2004), pp. 4635–4643.
[17] C. H. Choi and C. J. Kim, *Large slip of aqueous liquid flow over a nanoengineered superhydrophobic surface,* Phys. Rev. Lett., 96 (2006), 066001.
[18] K. Zhou and Y. Shang, *A parallel pressure projection stabilized finite element method for Stokes equation with nonlinear slip boundary conditions,* Adv. Appl. Math. Mech., 12 (2020), pp. 1438–1456.
[19] A. Maali and B. Bhushan, *Measurement of slip length on superhydrophobic surfaces,* Phil. Trans. Roy. Soc. A-Math. Phys. Eng. Sci, 370 (2012), pp. 2304–2320.
[20] P. Gilormini and H. Teyssedre, *On using the levelling of the free surface of a Newtonian fluid to measure viscosity and Navier slip length,* Proc. Roy. Soc. A-Math. Phys. Eng. Sci., 469 (2013), 20130457.
[21] J. Ou and J. P. Rothstein, *Direct velocity measurements of the flow past drag-reducing ultrahydrophobic surfaces,* Phys. Fluids, 17 (2005), 103606.
[22] V. John, *Slip with friction and penetration with resistance boundary conditions for the Navier-Stokes equations—numerical tests and aspects of the implementation,* J. Comput. Appl. Math., 147(2) (2002), pp. 287–300.
[23] V. A. Solonnikov and V. E. Shchadilov, *A certain boundary value problem for the stationary system of Navier-Stokes equations,* Trudy Mat. Inst. Steklova, 125 (1973), pp. 196–210.
[24] C. Amrouche and A. Rejaiba, *L^p-theory for Stokes and Navier-Stokes equations with Navier boundary condition,* J. Differ. Equ., 256 (4) (2014), pp. 1515–1547.
[25] C. Conca, *On the application of the homogenization theory to a class of problems arising in fluid mechanics,* J. Math. Pures Appl., 64 (1) (1985), pp. 31–75.
[26] H. Beirão Da Veiga, *Regularity for Stokes and generalized Stokes systems under nonhomogeneous slip-type boundary conditions,* Adv. Differ. Equ., 9 (9-10) (2004), pp. 1079–1114.
[27] P. Acevedo, C. Amrouche, C. Conca and A. Ghosh, *Stokes and Navier–Stokes equations with Navier boundary condition,* Comptes Rendus Mathematique, 357 (2019), pp. 115–119.
[28] P. Acevedo, C. Amrouche, C. Conca and A. Ghosh, *Stokes and Navier-Stokes equations with Navier boundary conditions,* J. Diff. Equ., 285 (2021), pp. 258–320.
[29] Le Roux C, *Flows of incompressible viscous liquids with anisotropic wall slip,* J. Math. Anal. Appl., 465 (2018), pp. 723–730.
[30] E. S. Baranovskii, *On flows of Bingham-type fluids with threshold slippage,* Adv. Math. Phys., 2017 (2017), 7548328.

[31] E. S. BARANOVSKII, *Steady flows of an Oldroyd fluid with threshold slip,* Commun. Pure Appl. Anal., 18 (2019), pp. 735–750.
[32] D. IFTIMIE AND F. SUEUR, *Viscous boundary layers for the Navier-Stokes equations with the Navier slip conditions,* Arch. Ration. Mech. Anal., 199 (1) (2011), pp. 145–175.
[33] N. MASMOUDI AND F. ROUSSET, *Uniform regularity for the Navier-Stokes equation with Navier boundary condition,* Arch. Ration. Mech. Anal., 203 (2) (2012), pp. 529–575.
[34] D. GILBARG AND N. S. TRUDINGER, Elliptic Partial Differential Equations of Second Order, Springer-Verlag, 2001.
[35] O. A. LADYZHENSKAYA, The Mathematical Theory of Viscous Incompressible Flow, Gordon & Breachm, 1969.
[36] Z. YAN, Low Reynolds Number Flow Theory (in Chinese), Peking University Press, 2002.
[37] M. I. G. BLOOR AND M. J. WILSON, *An approximate analytic solution method for the biharmonic problem,* Proc. Roy. Soc. A-Math. Phys. Eng. Sci, 462 (2006), pp. 1107–1121.
[38] H. QI, A. LIANG, H. JIANG, X. CHONG AND Y. WANG, *Effect of Pipe Surface Wettability on Flow Slip Property,* Indus. Eng. Chem. Res., 57 (2018), pp. 12543–12550.
[39] C. WANG, B. WEN, Y. TU, R. WAN AND H. FANG, *Friction reduction at a superhydrophilic surface: role of ordered water,* J. Phy. Chem. C, 119 (2015), pp. 11679–11684.
[40] T. A. HO, D. V. PAPAVASSILIOU, L. L. LEE AND A. STRIOLO, *Liquid water can slip on a hydrophilic surface,* Proc. Nat. Acad. Sci. U. S. A., 108 (2011), pp. 16170–16175.